Elicitation of potent serum neutralizing antibody responses in rabbits by immunization with an HIV-1 clade C trimeric Env derived from an Indian elite neutralizer

Rajesh Kumar [1§], Suprit Deshpande [1§], Leigh M. Sewall [2], Gabriel Ozorowski [2], Christopher A. Cottrell [2], Wen-Hsin Lee [2], Lauren G. Holden [2], Sara T. Richey[2], Antra Singh Chandrawacar [3,4], Kanika Dhiman [3], Ashish [3,4], Vivek Kumar [1], Shubbir Ahmed, Nitin Hingankar [1], Naresh Kumar, Kailapuri G Murugavel [5], Aylur K Srikrishnan [5], Devin Sok [6], Andrew B. Ward [2], Jayanta Bhattacharya [1, 7] *

1. Translational Health Science & Technology Institute, NCR Biotech Science Cluster, Faridabad, Haryana-121001, India
2. Department of Integrative Structural and Computational Biology, The Scripps Research Institute, La Jolla, CA 92037, USA; Scripps Consortium for HIV/AIDS Vaccine Development (CHAVD), The Scripps Research Institute, La Jolla, CA 92037, USA; IAVI Neutralizing Antibody Center and the Collaboration for AIDS Vaccine Discovery (CAVD), The Scripps Research Institute, La Jolla, CA 92037, USA.
3. CSIR-Institute of Microbial Technology (IMTECH), Chandigarh 160036
4. Academy of Scientific and Innovative Research (AcSIR), Ghaziabad 201002
5. Y. R. Gaitonde Centre for AIDS Research and Education, YRG CARE Laboratory, Rajiv Gandhi Salai, Adyar, Chennai-600113, Chennai, India, 600113;
6. IAVI Neutralizing Antibody Center, The Scripps Research Institute, La Jolla, CA 92037, USA; Department of Immunology and Microbiology, The Scripps Research Institute, La Jolla, CA 92037, USA; Consortium for HIV/AIDS Vaccine Development (CHAVD), The Scripps Research Institute, La Jolla, CA 92037, USA; International AIDS Vaccine Initiative (IAVI), New York, NY10004, USA.
7. International AIDS Vaccine Initiative, New Delhi - 110029, India; International AIDS Vaccine Initiative, New York, NY 10004, USA.

Running title: Structural and immunogenic properties of an HIV-1 clade C Env trimer

Key words: HIV-1, clade C, neutralizing antibodies, SOSIP, trimeric envelope, immunogenicity, elite neutralizer, electron microscopy

Abstract word count: 285

Competing interest:
An Indian provisional patent application filed jointly by THSTI and IAVI on the sequence and partial applications of the 1PGE-THIVC (Indian HIV-1 clade C trimer); Provisional Patent Application No: 201911036660 with the following inventors: Dr. Jayanta Bhattacharya, Dr. Rajesh Kumar, Mr. Vivek Kumar, Dr. Suprit Despande, Dr. Murugavel Kailapuri Gangatharan.

§ equal contribution

*** Corresponding author**:

E-mail: JBhattacharya@iavi.org; JBhattacharya@thsti.res.in

Abstract

Evaluating the structure-function relationship of viral envelope (Env) evolution and the development of broadly cross-neutralizing antibodies (bnAbs) in natural infection can inform rational immunogen design. In the present study, we examined the magnitude and specificity of autologous neutralizing antibodies induced in rabbits by a novel HIV-1 clade C Env protein (1PGE-THIVC) *vis-à-vis* those developed in an elite neutralizer from whom the *env* sequence was obtained that was used to prepare the soluble Env protein. The thermostable 1PGE-THIVC Env displayed a native like pre-fusion closed conformation in solution as determined by small angle X-ray scattering (SAXS) and negative stain electron microscopy (EM). This closed spike conformation of 1PGE-THIVC Env trimers was correlated with weak or undetectable binding of non-neutralizing monoclonal antibodies (mAbs) compared to neutralizing mAbs. Furthermore, 1PGE-THIVC SOSIP induced potent neutralizing antibodies in rabbits to autologous virus variants. The autologous neutralizing antibody specificity induced in rabbits by 1PGE-THIVC was mapped to the C3/V4 region (T362/P401) of viral Env. This observation agreed with electron microscopy polyclonal epitope mapping (EMPEM) of the Env trimer complexed with IgG Fab prepared from the immunized rabbit sera. While the specificity of antibodies elicited in rabbits associated with neutralizing autologous viruses were distinct to those developed in the elite neutralizer, EMPEM analysis demonstrated significant changes to Env conformations when incubated with polyclonal antibody sera from the elite neutralizer, suggesting these antibodies lead to the destabilization of Env trimers. Our study not only shows distinct mechanisms associated with potent neutralization of sequence matched and unmatched autologous viruses by antibodies induced in rabbits and in the elite neutralizer, but also highlights how neutralizing antibodies developed during the course of natural infection can impact viral Env conformations.

Author Summary

The interplay between circulating virus variants and broadly cross neutralizing polyclonal antibodies developed in a subset of elite neutralizers is widely believed to provide strategies for rational immunogen design. In the present study, we studied the structural, antigenic and immunogenic properties of a thermostable soluble trimeric protein with near native pre-fusion conformation prepared using the primary sequence of an HIV-1 clade C *env* isolated from the broadly cross neutralizing plasma of an elite neutralizer. This novel SOSIP Env trimer demonstrated comparable antigenic, structural and immunogenic properties that favoured several ongoing subunit vaccine design efforts. The novel clade C SOSIP induced polyclonal neutralizing antibody response developed in rabbits not only differed in its epitope specificity compared to that elicited in natural infection in presence of pool of viral quasispecies but also showed how they differ in their ability to influence Env structure and conformation. A better understanding of how vaccine-induced polyclonal neutralizing antibody responses compares to responses that developed in natural infection will improve our knowledge in designing better vaccine design strategies.

Introduction

The elicitation of protective immune response by vaccination to protect against the enormous genetic diversity of HIV remains a challenge (1-5). Envelope (Env) spikes, which facilitate HIV entry and establish infection, are being considered as candidate immunogens because they mimic the trimer spike on virions (6-9). A number of recently published studies have demonstrated how structure guided stabilized Env trimers can induce potent neutralizing antibodies in different animal models (10-22). In addition, Env trimers have been used as antigen baits for the isolation bnAbs by B cell sorting and enabled structural characterization of antibody epitopes on Env (16, 23-27). Although in general, most of the trimeric Envs with closed conformation elicitated of neutralizing antibodies to tier-1 and tier 2 sequence matched autologous viruses in different animal models, their target specificities varied subtly (14, 19, 28-31). As the quality and specificity of different Env trimer-induced neutralizing antibody responses varies, presumably because of difference in the *env* sequences used to prepare the trimeric Env proteins, there is value in producing additional recombinant HIV trimers from different clades, particularly those isolated from individuals who developed broadly neutralizing antibodies. We previously reported characterized genetic and neutralization properties of *env* sequences obtained from an Indian elite neutralizer (G37080) whose plasma antibodies demonstrated >90% neutralization breadth when tested against a large heterologous Env-pseudotyped virus panel (32).

In the present study, we examined the structural, antigenic and immunogenic properties of an HIV-1 trimeric Env SOSIP protein (referred to as 1PGE-THIVC) prepared using the sequence of one of the autologous *envs* (PG80v1.eJ19) obtained from an elite neutralizer. The autologous virus is sensitive to some existing bnAbs and plasma neutralizing antibodies developed in this individual as reported earlier, but not to non-neutralizing antibodies and sCD4 (32, 33). Our overall goal in this study was to compare differences in antibody responses between immunization with recombinant 1PGE-THIVC in rabbits and those that develop during natural infection course. Three of the four rabbits immunized with the highly stable, well-ordered near native 1PGE-THIVC with closed conformation and with desirable antigenicity elicited neutralizing antibodies that demonstrated potent neutralization of tier-2 autologous virus variants, including one highly resistant *env*

(PG80v2.eJ38) that was associated with escape from humoral antibody response mounted in the elite neutralizer (32, 33). Notably, neutralizing antibodies induced in rabbits by 1PGE-THIVC targeted discontinuous amino acids in the C3/T362 and V4/P401 regions on viral Env, which are distinct from those reported earlier for other Env SOSIPs. Epitopes at the C3/V4 region of HIV-1 Env targeted by SOSIP-induced neutralizing antibodies in rabbits and guinea pigs have also been previously reported (16, 34), however their antibody-specificity differed to what we have observed in this study. Moreover, we did not find (28, 29, 35) glycan holes associated with induction of SOSIP-induced neutralizing antibody response (34) in our study. The neutralizing antibody specificity developed in rabbits, however, was distinct to the kind elicited in the elite neutralizer from whom 1PGE-THIVC primary sequence was obtained.

Results

Characterization of an HIV-1 clade C Env trimer obtained from an Indian elite neutralizer.

We previously reported an Indian elite neutralizer (G37080) infected with HIV-1 clade C whose plasma antibodies demonstrated neutralization of over 90% of a cross-clade pseudotyped virus panel (32). Additionally, we reported the degree of susceptibility of pseudotyped viruses expressing primary *envs* obtained from G37080 donor to both autologous plasma antibodies as well as different neutralizing and non-neutralizing mAbs (32, 33). One of these autologous *envs*, PG80v1.eJ19, when expressed as pseudotyped virus was susceptible to a range of neutralizing antibodies but not to sCD4 or to non-neutralizing mAbs, including V3 epitopes (3074 and 3896), b6, F105 and 17b (33). This Env was also resistant to PGT121, PGT128 and PGT135 bnAbs presumably due to natural absence of N332 at the V3 base (33). Interestingly, in contrast to all other autologous Envs, PG80v1.eJ19 was the only variant that was naturally sensitive to PGT145 (33) and hence was selected for preparation as a recombinant SOSIP trimer (1PGE-THIVC). PGT145 exclusively binds to a conformational epitope on trimeric Env, thus providing advantages in purifying pure and near native soluble Env trimers via affinity chromatography (36). Codon optimized 1PGE-THIVC SOSIP was designed, expressed in 293F or Expi293 cells and trimeric fractions were purified by PGT145 affinity column followed by size exclusion chromatography (SEC) (Figure 1A & B). The 1PGE-THIVC SOSIP assembled as >95% well-ordered trimer populations by 2D negative stain EM (Figure 1D). While 1PGE-THIVC showed a single gp140 band in SDS-PAGE (Figure 1C), the trimer converted into gp120 in the presence of DTT under reducing condition in SDS-PAGE (Figure 1E). One of the hallmarks of trimeric Envs that preferentially binds to neutralizing antibodies is that they tend to be efficiently cleaved compared to uncleaved or partially cleaved Envs, which generally expose non-neutralizing epitopes (13, 37-39). Our data indicated that the antigenicity of 1PGE-THIVC was correlated with the soluble trimers being efficiently cleaved.

We next examined the conformational stability of the 1PGE-THIVC Env trimer. First, we assessed the antigenicity of 1PGE-THIVC Env by measuring binding to neutralizing and non-neutralizing mAbs by ELISA

(avidity). To facilitate binding with mAbs in trimeric state, D7324 epitope was introduced in the C- terminus in 1PGE-THIVC as described before (40). As shown in Figure 2A, 1PGE-THIVC preferentially bound to neutralizing mAbs over non-neutralizing mAbs. The binding affinity of 1PGE-THIVC to neutralizing and non-neutralizing mAbs with distinct specificities was next examined by BLI-Octet analysis (Figure 2B). For assessing binding affinity to bnAbs, we selected VRC01 and those that are dependent on quaternary conformation e.g., PG9, PGT145 and PGDM1400. VRC01, which targets the CD4bs, bound to 1PGE-THIVC with a very fast on-rate and very slow dissociation during wash and resulted an affinity of less than 1 nM (*KD* 1.7 nM). 1PGE-THIVC also bound strongly to PGT145 and PGDM1400 with affinities (KD) of 14 nM and 29 nM respectively (Figure 2B). Relative to PGT145 and PGDM1400, 1PGE-THIVC showed weak binding to PG9 bnAb, which also targets conformational epitopes including glycans in V1V2, with a KD of 41 nM (Figure 2B). Interestingly, the increased binding of 1PGE-THIVC to both VRC01 and CD4-Ig was found to be dependent on Asn279 (not a PNGS) on viral Env and also showed evidence in our study to significantly reduce formation of sCD4-induced higher oligomer as observed in blue native PAGE (Figure 3). We noted that the highly conserved Asn276 (glycan) is also present in 1PGE-THIVC. As expected, and in line with what we observed in binding ELISA, 1PGE-THIVC did not bind to the non-neutralizing mAb F105. Taken together, these observation results suggested that the antigenic properties of the soluble PG80v1.eJ19 SOSIP.664 Env is consistent with those expected of a well-ordered native like Env trimers as the trimer binds to neutralizing bnAbs with high affinity and has limited binding to non-neutralizing antibodies.

We next examined the thermostability of the 1PGE-THIVC Env trimers by measuring the melting temperature (*Tm*) using differential scanning calorimetry (DSC). As shown in Figure 4A, the *Tm* for 1PGE-THIVC was observed to be approximately 62°C with an onset of melting at approximately 55°C. The high *Tm* obtained for the 1PGE-THIVC was comparable with the double cysteine mutant reported stable Env trimers like BG505.SOSIP.664 (13) and LT5.J4b12C SOSIP.664 (40). The soluble 1PGE-THIVC was also found to demonstrate stability at 37°C as measured by its ability to bind to different bnAbs by D7324-ELISA (Figure 4B). Overall, our data suggested that the soluble 1PGE-THIVC efficiently expresses highly stable well-ordered

trimers in a closed conformation, which predominantly occludes epitopes that are targets of non-neutralizing antibodies.

Structural properties of the trimeric 1PGE-THIVC Env as determined by Small-angle X-ray scattering (SAXS) and homology modeling.

The SAXS I(q) profile of 1PGE-THIVC at concentration of 0.85 mg/ml is presented in Figure 5. The data is shown in double logarithm mode and confirms a monodisperse sample profile that lacks any aggregation or interparticulate effects. Of all the acquired data points collected (black squares), the used data points are shown in blue color. Kratky plot of the dataset show a clear peak profile supporting a globular scattering profile of the protein molecules in solution (lower inset). Distribution of interatomic vectors show that the SOSIP molecules have a maximum linear dimension (D_{max}) of about 15 nm with radius of gyration (R_g) of 5.1 nm. The representative SAXS profile based on the estimation is shown as a red line in Figure 5A. The calculated SAXS data-based model of 1PGE-THIVC SOSIP molecule is shown in Figure 5B. The common envelope to all models is shown as map and the variation amongst ten models is shown as blue mesh. Normalized spatial disposition (NSD) amongst the ten models was 0.762 suggesting high similarity between the solutions. To compare this SAXS based model with previously determined structure of SOSIP, we used the primary structure of 1PGE-THIVC to generate a homology model of the protein (the closest template was PDB 6B0N) (shown as red, blue and green ribbons in Figure 5B). PDB 6B0N is crystal structure of prefusion state of HIV Env glycoprotein trimer of the clade A BG505 isolate in complex with Fabs of PGT122 and PGV19 (41). The sugar moieties of PDB 6B0N shown as magenta sticks were borrowed as such to represent glycosylation in 1PGE-THIVC. The homology model was inertially aligned over the SAXS based envelope. Three orthogonal views of the superimposition are shown in Figure 5B and 5C which provide visual confirmation that 1PGE-THIVC is also folded in P3 symmetry in same size/shape profile as previous models. Side-view shows that in the inertially aligned models, the SAXS data-based Env is not occupied in the bottom or gp41 side of the homology model (indicated by arrow). Using the SAXS and homology-based model, the different stretches of 1PGE-

154 THIVC SOSIP as determined by SAXS and homology-based model is shown in Figure S1 (supplementary
155 data).
156
157 **1PGE-THIVC Env induced potent neutralizing antibodies against sequence matched and unmatched**
158 **tier-2 autologous Envs.**
159
160 In line with the favorable antigenic properties demonstrated 1PGE-THIVC, which is expected of well-ordered
161 Env trimers, we next examined its ability to induce neutralizing antibodies in rabbits. Four New Zealand female
162 white rabbits were primed and boosted with 1PGE-THIVC trimers along with Quil-A adjuvant. Two rabbits
163 were given PBS throughout the study as control group. Quil-A was selected as an adjuvant as it was reported
164 to stimulate the antibody-mediated immune responses against range of antigens including viruses (42),
165 modulates antibody fine-specificity (43) and does not alter the conformation when mixed with HIV-1 Env
166 trimers (44). The prime-boost schedule used in the process of rabbit immunization is shown in Figure 6A.
167 Rabbits were bled before initiation of immunization (day 0) and at week 2 post priming and at weeks, 6, 8 and
168 12 post first boost and weeks 22, 24 and 28 following second boost with mixture of 30 µg of SOSIP protein
169 and 40µg of Quil-A as indicated in Figure 6A. Serum samples prepared from blood samples collected at
170 indicated intervals were heat-inactivated at 56°C for 1 hour to deactivate complement. Subsequently, the sera
171 were evaluated for binding to 1PGE-THIVC by D7324 capture ELISA (Figure 6B) and neutralization of
172 pseudotyped viruses expressing sequenced-matched autologous *envs* (PG80v1.eJ19 and PG80v1.eJ19 T332N)
173 (Figure 6C & D) and two heterologous Tier 1 *envs (*SF162 and 93IN905). The peak binding of 1PGE-THIVC
174 to serum antibodies was demonstrated by serum samples collected at week 10 and beyond from the immunized
175 rabbits (Figure 6C). Serum samples from week 22 that demonstrated optimal binding to 1PGE-THIVC as
176 demonstrated by D7324 ELISA was subsequently examined for its ability to neutralize sequence matched
177 autologous Env-pseudotyped virus (PG80v1.eJ19). As shown Table 1, serum antibodies potently neutralized
178 pseudoviruses expressing both the sequence matched (PG80v1.eJ19 and PG80v1.eJ19 T332N) and sequence
179 unmatched (PG80v1.eJ7, PG80v1.eJ17, PG80v1.eJ158 and PG80v2.eJ38) autologous *envs*. We observed

potent neutralization of PG80v2.eJ38, which was unexpected as this Env is not only resistant to autologous donor plasma antibodies (32) obtained from this elite neutralizer but also highly resistant (much like a tier-3 Env) to several bnAbs (33). Such observation was not reported earlier with any SOSIP-induced neutralizing antibodies to the best of our knowledge. Additionally, although modest neutralization of heterologous Tier 1 Env-pseudotyped viruses (SF162 and 93IN905) was observed, however with lower magnitude compared to autologous viruses (Figure 6E, F, H), which was possibly due to trimer falling apart thereby exposing the immunodominant epitopes in V3 region. Towards confirming the specificity of antibody-mediated virus neutralization, when tested, purified rabbit serum IgG was found to show neutralization of pseudoviruses expressing autologous *envs* in a dose-dependent manner (Figure 6H); thus, confirming the concordance of serum (Figure 6G) versus serum IgG mediated virus neutralization. Finally, potent autologous neutralization was correlated with efficient binding of serum IgG with 1PGE-THIVC SOSIP (Figure 6I). Taken together, our results indicated that 1PGE-THIC SOSIP trimers was able to induce antibodies in rabbits that demonstrated potent neutralization of pseudoviruses expressing sequence matched and unmatched tier-2 Envs and also demonstrated some degree of heterologous neutralization as well.

Mapping target epitope specificities of neutralizing antibodies elicited in rabbits induced by 1PGE-THIVC.

We next examined the target specificity of the antibodies that demonstrated potent neutralization of autologous Env-pseudotyped viruses. Serum sample obtained at week-24 from rabbit #1 which demonstrated maximal and potent neutralization of autologous Envs was used to map epitope specificities using the pseudoviruses expressing wild type, chimeric and mutant autologous *env* constructs. Chimeric autologous envelope constructs were prepared between sensitive (PG80v1.eJ7 and PG80v1.eJ19) and this resistant autologous envelope (PG80v2.eJ38) as was done to assess specificities of human plasma antibodies too as shown above. As shown in Table 2, the resistant PG80v2.eJ38 Env-pseudotyped virus expressing V3/C4 sequence swapped from the sensitive PG80v1.eJ7 *env* was neutralized by serum antibodies in contrast to its wild type form, suggesting that

the antibodies induced in rabbits by 1PGE-THIVC mediated potent neutralization of autologous viruses by targeting epitopes in the V3/C4 region of the viral Env. To further map its fine specificities, we prepared and tested mutant *env* constructs in the PG80v2.eJ38 backbone. We found that substitutions of amino acids asparagine (glycan) with threonine at the 362 position (N362T) in the C3 and leucine to proline at the 401 position (L401P) in the V4 regions resulted in over 8-fold increase in neutralization sensitivity (Table 2 and Figure S2) of the PG80v2.eJ38 Env-pseudotyped virus compared to its wild type form. Also, as shown in Table 2, combination of T362N and P401L substitutions resulted in over 17 and 12- fold resistance of pseudotyped viruses expressing PG80v1.eJ7 and PG80v1.eJ19 *envs* respectively having similar C3/V4 protein sequence (Figure S2) compared to their wild type forms. Interestingly, while single substitutions of T362N and P401L in PG80v1.eJ19 *env* demonstrated reduction in virus neutralization by 5.28 and 6.26-fold respectively, the combination of both demonstrated a substantial reduction in virus neutralization as described above, indicating that T362 and P401 likely comprises an epitope in the C3/V4 region targeted by neutralizing antibodies induced in rabbits. Finally, as shown in Figure 7, compared to undepleted serum, we observed a significant reduction in the neutralization of pseudoviruses expressing autologous *envs* by 1PGE-THIVC trimer- depleted serum. Taken together, our results indicate that 1PGE-THIVC SOSIP developed using a primary *env* sequence amplified from an Indian elite neutralizer induced potent autologous neutralizing antibodies in rabbits having target epitope specificities to the C3/V4 epitope on trimeric Env, which is distinct to both autologous and heterologous broadly neutralizing antibodies developed in the elite neutralizer (Table S1).

Mapping polyclonal antibody specificities by ns-EMPEM analysis.

The rabbit polyclonal serum antibody specificities developed over time following 1PGE-THIVC immunization were further examined by analyzing trimer-Fab complexes by EMPEM (45) (Figure 8). Trimer-specific responses were already observed at week 6 (2 weeks following the first boost), although against epitopes that are often seen in soluble Env immunizations and are considered non-neutralizing. These two responses are against the base of the trimer, which would not be inaccessible in a full-length native Env, and a region that coincides with the N611 glycan. Antibodies that target the N611 glycan have not been described, however

recent work reveals that this site is under-occupied (i.e. it contains the correct PNGS consensus sequence, but the asparagine is glycosylated to a varying degree) in certain recombinantly expressed, engineered Env trimers, creating a neoepitope that is not believed to exist on native Env (46). These two non-neutralizing responses persist in later timepoints. By week 12 (8 weeks following the first boost) a third response is detected in the vicinity of the C3/V5 epitope. This is in agreement (and presumably the same response) as the C3/V4 epitope described above. Antibodies against this epitope have been described and tend to be potent autologous neutralizers with limited cross-reactivity. Finally, at week 22 (2 weeks following the second boost) a fourth epitope is detected by EMPEM against the region comprised of V1/V3 and/or V2 (the resolution of negative stain EM cannot discern such subtleties). This response may share some overlap with bnAbs that target the V3-glycan epitope, although the lack of heterologous neutralization by the serum implies that these antibodies rely heavily on the variable regions of Env and are more strain specific.

Evidence of destabilization of SOSIP trimer conformation by autologous polyclonal antibodies elicited during natural infection course in the elite neutralizer (G37080).

We next examined the impact of polyclonal plasma antibodies on the conformational state of the 1PGE-THIVC trimers. Thus, as a comparison to the EMPEM analysis we carried out with rabbit serum as described above, we also analyzed the polyclonal IgG isolated from this chronically infected human elite neutralizer that demonstrated broad cross-clade neutralization (32). Digested Fab prepared from polyclonal plasma samples were used to prepare grids with the trimer-Fab complexes as monodisperse particles. As shown in Figure 9, contrary to the rabbit immunization experiment, in which a defined set of epitopes were observed against the trimer, the EM results for the human polyclonal plasma antibodies showed a high level of heterogeneity. 2D classification revealed heterogeneity in trimer-Fab complex, in which the majority of the classes appear to be Env protomers decorated with multiple Fabs or non-native open trimers. In fact, most of the 2D class averages reveal clusters of Fabs bound to fragments of Env, with no clear indication that intact trimers are part of these complexes. In the single 2D class containing an intact trimer, no Fabs are bound (Figure 9B). These data suggest

that the human donor developed antibodies that recognize multiple epitopes and were likely associated with destabilization of the engineered Env trimer ectodomain. The particles from the 2D classes do not reconstruct into an interpretable 3D density when provided a closed and ligand-free trimer as the initial model, which is likely a result of trimer dissociation (classes represent free protomers with several Fabs bound), trimer opening, or a combination of both. At least two broadly-neutralizing antibodies have been reported that induce trimer dissociation by targeting gp41, 3BC315 (derived from natural human infection) (47), and 1C2 (derived from rabbit immunization with engineered Env) (48). It has also been reported that antibodies directed against the CD4 binding site, V3 loop and the MPER can induce gp120 shedding (49). More recently, a study revealed that some V3 loop-targeting macaque antibodies can neutralize certain tier 2 viruses but require open conformations of Env with V3 exposed (50). While we are not able to assign specific epitopes from the EM data, it is clear that the responses during natural infection vary greatly comparted to the rabbit immunization study.

Discussion

While near-native soluble Env trimers have been described by other studies, it remains unclear how viral envelopes obtained from individuals who developed broadly cross neutralizing antibody responses in the course of natural infection can contribute to the elicitation of bnAbs by vaccination (19). The autologous neutralizing antibody response driving virus escape is an important step towards the initiation of a cascade of viral and B cell evolutionary events resulting in the development of potent and broad neutralizing antibodies in certain individuals. Investigating the quality, magnitude and specificity of the neutralizing antibody responses induced by geographically divergent *env* sequences obtained from elite neutralizers would likely provide key strategic clues in better formulating HIV immunogens for eliciting the desired vaccine-induced protective antibody responses. Attempts have been made to examine antigenic and immunogenic properties of Env trimers prepared from *env* sequences obtained from elite neutralizers (20, 60, 61). The near native 1PGE-THIVC SOSIP soluble trimeric gp140 protein prepared using the wild type (native) *env* sequence from the Indian elite neutralizer was found not only to express very efficiently but also demonstrated the elicitation of potent autologous tier-2 neutralizing antibodies in rabbits.

The rationale for selecting the clade C PG80v1.eJ19 sequence to prepare the 1PGE-THIVC SOSIP trimer is due to its sensitivity to neutralizing and resistance to all non-neutralizing antibodies tested including those that target coreceptor binding sites, sCD4 (33) and donor serum antibodies, which indicated that the viral envelope has favorable properties that might mimic the closed pre-fusion conformation. In the present study, we sought to examine how neutralizing antibodies induced in rabbits by 1PGE-THIVC representing PG80v1.eJ19 compare in their specificity, magnitude and quality with those elicited during the course of infection in this elite neutralizer.

Before initiating the rabbit immunization, we confirmed that the thermostable 1PGE-THIVC demonstrated favorable biophysical, biochemical, antigenic and structural properties. Without any additional modification, efficient expression of trimeric Envs was observed following PGT145 affinity purification and the trimer also showed closed near native conformation by low resolution negative stain EM analysis. Moreover, an Asn279Glu substitution was found to enhance binding of the trimer to VRC01 without promoting

CD4-induced conformational rearrangement that results in the open conformation of Env, which is known to expose unwanted immunodominant epitopes and induce non-neutralizing antibody response following immunization. It is intriguing that substitution of Asn279Glu, which is a part of the loop D, is very conserved (www.hiv.lanl.gov) and also forms a contact site for CD4bs directed mAbs such as HJ16 and VRC01 (62-64), demonstrated enhanced binding of 1PGE-THIVC trimer to VRC01. Removal of Asn279 position (N279) was previously shown to demonstrate detrimental effect on recognition of VRC01 class antibodies (65). The 279 position in the gp120 loop D is predominantly occupied by either Asn or Asp (www.hiv.lanl.gov) and recently was reported by LaBranche *et al.* (64) that Asn279Lys along with Gly458Tyr mutations conferred transmitted/founder virus and Env protein with enhanced susceptibility to antibodies representing germline antibodies.

We also report on how the 1PGE-THIVC folds and breathes in solution under non-frozen conditions. One of the reasons why we were keen to examine how the SOSIP trimer 1PGE-THIVC behaves in solution was to predict the conformation expected *in vivo* in circulation post rabbit immunization. The SAXS data indicated that the 1PGE-THIVC SOSIP is folded in P3 or 3-fold symmetry however retains some degree of inherent molecular mobility/disorder which possibly could result in influencing recognition by neutralizing antibodies.

The 1PGE-THIVC immunized rabbit sera neutralized pseudoviruses expressing both sequence matched and unmatched autologous *envs*. These autologous envelopes obtained from the plasma sample of the elite neutralizer at the baseline visit, although sensitive to the follow up plasma neutralizing antibodies obtained from this donor (32), were resistant to non-neutralizing mAbs including those that target the V3 immunodominant epitopes (such as 3074 and 3869) and the coreceptor binding site (e.g., 17b) (33). Interestingly, serum antibodies obtained from two immunized rabbits (rabbit # 1 and rabbit # 4) were found to show modest neutralization of the autologous PG80v2.eJ38 env that showed complete resistance to human plasma antibodies obtained in the follow up visit from the elite neutralizer (32) and to several neutralizing and non-neutralizing mAbs (33), a property that is expected of envelopes of Tier 2/3 category. Previously, we reported that PG80v2.eJ38 escaped plasma autologous plasma antibodies by mutations in V1V2 region (32);

however did not distinguish the different antibody classes circulating in this elite neutralizer. In the present study, we dissected the antibody class developed in this elite neutralizer by distinguishing their specificities by depletion assays and found that the class that demonstrated exclusive autologous neutralization also had V1V2 specificity. These findings further confirmed our earlier observation of autologous virus escape by mutations in V1V2 region. In the present study, the immunized rabbit serum antibody specificity associated with neutralization of autologous viruses was mapped to C3/V4 specificity, which is distinct to the responses observed for human plasma neutralizing antibodies described above. Interestingly, although the N362 glycan residue present in the PG80v2.eJ38 *env* associated with some resistance to rabbit antibodies (and hence used for preparing chimeric env constructs for mapping antibody specificity), all were found to neutralize pseudovirus expressing PG80v2.eJ38 *env* except for the serum sample obtained from rabbit # 3. This observation is in sharp contrast to that observed with human plasma antibodies obtained from the elite neutralizer (32), which indicated that presence of proline residue at the 401 position in the C4 region possibly played a compensatory role that resulted in the neutralization of this tier 2/3 envelope. The 1PGE-THIVC induced antibodies in rabbits with C3/V4 specificity neutralized autologous virus (pseudotyped virus expressing PG80v2.eJ38) that was highly resistant to autologous human plasma antibodies as reported earlier (32), albeit with lower magnitude. Interestingly, the wild type PG80v1.eJ19 *env* lacks a glycan residue at the 332 position (N332) in the V3 base, instead contain threonine (T332). While preparing 1PGE-THIVC, we incorporated T332N, however it did not appear to induce N332 directed antibodies, neither did it improve sensitivity of the PG80v1.eJ19 T332N envelope to rabbit sera over PG80v1.eJ19 T332 envelope. We are unable to comprehend the basis for resistance of PG80v1.eJ19 T332N envelopes to serum samples obtained at week 22 from rabbit # 2 and 3 while the same sera neutralized pseudovirus expressing the PG80v1.eJ19 T332 *env*.

Despite production and *in vitro* characterization of well-ordered native like Env trimers, one of the concerns that remains post immunization is the stability and the ability of the Env trimers to retain its integrity *in vivo* as subtle distortion in conformation can lead to the induction of non-neutralizing antibodies via off-target binding. Loss in virus neutralization by trimer-depleted serum antibodies indicated that 1PGE-THIVC induced autologous neutralizing antibodies conformational epitopes. Indeed, serum antibodies obtained at week

22 from the rabbit that demonstrated the most potent neutralization also neutralized heterologous envelopes including those are categorized as Tier 1A. The magnitude of heterologous neutralization also differed; for example, SF162 and MW965 which are of Tier 1A category (66) showed maximal neutralization sensitivity compared to 93IN905 envelope which is of Tier 1B category (14). Intriguingly, this was not noticed with serum samples obtained from early time points post immunization. It is also important to note that the tier-2 clade A envelope, Q259.d2.17 was neutralized by the same serum antibodies at the same time. Therefore, it is unknown whether the neutralization of Tier 1 envelopes was exclusively mediated by non-neutralizing (such as those are directed to immunodominant V3 epitopes).

To further understand the quality of polyclonal antibodies developed in immunized rabbits, the polyclonal antibody imaging approach by negative stain EM analysis was carried out with serum samples collected at weeks 6 and 12 following first protein boost and at week 22 following second protein boost. The common feature of all these three serum samples is the presence of two non-neutralizing responses; gp41 base and a N611 glycan hole. The former is seen in majority of the soluble trimers that have been examined as this high peptide content base is highly immunogenic. The sub-occupancy of a glycan at position N611 has been demonstrated in BG505 SOSIP using mass spectrometry and cryo-EM (46). The N611 PNGS is highly conserved across clades (www.hiv.lanl.gov) and both PG80v1eJ19 and 1PGE-THIVC contain the consensus sequence for glycosylation at this position N611. While this is believed to be true for soluble SOSIP Env proteins, it is necessarily not true for primary viruses (67). Interestingly, in contrast to BG505 SOSIP, which demonstrated elicitation of strong 241/289 “glycan hole” directed antibody responses in rabbits (35), our data suggest that 1PGE-THIVC Env while this clade C *env* sequence naturally blocks those glycan epitopes. Additionally, rabbit sera also neutralized the pseudotyped virus expressing both parental PG80v1.eJ19 *env* having T332 and also its T332N version (Table 1), further indicating that neutralizing antibodies induced in rabbits also did not target N332 glycan epitope too. The serum samples collected at weeks 12 and 22 demonstrated a C3/V5 directed antibody response, similar to previously published reports (34). This epitope is predicted to be dependent on glycan repositioning in the V5 loop, and since the V5 glycosylation site(s) vary across genotypes, cross-reactivity is likely to be hampered as described very recently (68). Finally, the serum

sample collected at week 22 following second SOSIP boost demonstrated a fourth antibody response by nsEMPEM analysis that indicated "V1/V3" and "V2-like" antibody responses, which at low resolution (2D classification) remains difficult to distinguish. However, it should be noted that neither responses appeared the same as that of canonical bnAb "V1/V2-apex" or "V3-glycan supersite." We believe therefore that these antibodies will potentially have high levels of strain specificity as they interact with the V1, V2 and/or V3 variable regions. Of note 1PGE-THIVC SOSIP trimers appear "more open" at the apex in the 3D reconstructions compared to BG505 SOSIP. What this means immunologically is hard to say since there do not appear to be responses to newly exposed epitopes, nor are epitopes of the four distinct antibodies responses measured against 1PGE-THIVC SOSIP known to induce opening. The V3 signal observed in nsEMPEM could partially explain neutralization of tier 1 envelopes, however, neither neutralization of tier 1 envelopes was observed with serum samples up to week 12 post SOSIP boost nor any elicitation of V3 directed antibody observed by polyclonal EMPEM analysis. Interestingly, in contrast to the specificities of neutralizing antibodies induced in rabbits as observed by EMPEM analysis, broadly cross neutralizing polyclonal antibodies developed in the human elite neutralizer drastically altered the trimer conformation of the sequence matched antigen that was used for rabbit immunization. While such observation has not been documented previously in the context of polyclonal antibody mapping, our observation indicates that a population of antibodies in the polyclonal mixture, possibly correlated to the broad neutralization developed in this elite neutralizer, are capable of destabilizing trimers, exposing additional epitopes that are normally buried surfaces (for example though gp120-induced shedding in natural infection) as shown in other unrelated studies (47, 49). This clearly suggests that the neutralizing antibody responses induced in rabbits by 1PGE-THIVC SOSIP trimer are different than those elicited during the course of natural infection in this individual. Although not known definitively, such phenomenon may possibly be linked with development of virus-antibody co-evolution leading towards achieving neutralization breadth. While in contrast to the rabbit antibodies, we could not infer human polyclonal antibody specificity by EMPEM, our data highlights how antibodies developed in natural infection that are tied neutralization breadth can significantly impact upon Env conformation. It would be important to further investigate the mechanism underlying this phenomenon by examining virus and

401 antibody interaction by following individuals infected with HIV overtime, particularly those who go on to
402 develop cross neutralizing antibodies in the course of natural infection. In summary, it is important to study
403 different well-ordered native SOSIPs in different animal models, which would better inform what structural,
404 antigenic and immunogenic properties can better guide and select Env SOSIPs that would likely to help achieve
405 neutralization breadth to genetically diversified HIV. Moreover, since subtype C accounts for nearly half of the
406 global HIV infection (www.hiv.lanl.gov), it is important to select and study region-specific HIV-1 Envs (e.g.,
407 clade C) and which are associated with mounting neutralizing antibodies *in vivo* in the natural infection course.
408 Such exercise will likely be able to inform the rational design and development of immunogens that can least
409 be able to largely dissect the region-specific diversity of circulating HIV-1 subtypes such as clade C.

410

411 **Materials and Methods**

412

413 **Ethics Statement.**

414 The blood samples were collected under the IAVI Protocol G study from slow-progressing ART naive HIV-1-
415 positive donors from Nellore District of the state of Andhra Pradesh, southern India, by trained clinicians at the
416 YRG Care Hospital following approval and clearance from the Institutional Review Board (IRB) and the Ethics
417 Committee. The plasma samples collected were shipped to the Translational Health Science and Technology
418 Institute, for research purpose only. The rabbit immunization work was outsourced to a contract research
419 organization that obtained necessary approvals from animal ethics committee prior to conducting immunization
420 and collecting blood samples from vaccinated rabbits.

421

422 **Preparation of** 1**PGE-THIVC SOSIP trimer.**

423 Codon optimized HIV-1 Indian clade C (1PGE-THIVC) gp140 SOSIP trimeric protein was prepared based on
424 a Tier-2 HIV-1 clade C primary *env* sequence (PG80v1.eJ19), obtained from an Indian elite neutralizer (32)
425 essentially as described by Sanders *et al*. (13). 1PGE-THIVC gene was codon-optimized by GeneArt (Thermo
426 Fisher Inc.) and cloned into pcDNA3.1(+) with following modifications to the wild-type Env sequence: A501C,
427 T605C, I559C (for trimer stabilization), and gp120 - gp41 cleavage motif REKR changed to RRRRRR. The
428 D7324 epitope sequence (GSAPTKAKRRVVQREKR) was added after residue 664 in gp41 ectodomain
429 (ECTO) and preceding the stop codon to facilitate examining Env SOSIP binding by ELISA following
430 published protocol (40, 51). 1PGE-THIVC was expressed by transient transfection of 293F or Expi293 cells,
431 and the trimeric protein fraction was purified from culture supernatants first by using PGT145 mAb affinity
432 column (36). Bound proteins were eluted with 3 M $MgCl_2$, dialyzed with PBS pH (7.4), and subsequently
433 concentrated using Amicon ultracentrifuge filters (Millipore) with a 100-kDa cutoff to 0.5-1 ml. The PGT145
434 affinity purified SOSIP protein was further subjected to size exclusion chromatography (SEC) using a HiLoad
435 Superdex 200 16/60 column (GE Healthcare Inc.). The SEC purified proteins were snap frozen in liquid
436 nitrogen and stored at -80°C until further use. Purified trimeric SOSIP proteins were analyzed in a gradient 4-

15% BN-PAGE (Mini-PROTEAN TGXTM, Bio-Rad). The degree of 1PGE-THIVC cleavage was examined by incubating the SOSIP protein with 0.1 M dithiothreitol (DTT) and analyzed by SDS-PAGE under reducing conditions as described earlier (40).

Trimer ELISA

Binding of SOSIP trimers to different mAbs by D7324 sandwich ELISA was carried out as described previously (40). Briefly, high-binding microtiter plates (Nunc, Inc.) were first coated with D7324 antibody (Aalto Bio Reagents, Dublin, Ireland) at 10 µg/ml (100 µl/well) in coating buffer (150 mM Na_2CO_3, 350 mM $NaHCO_3$, 30 mM NaN_3, pH 9.6) at 4°C overnight. Microtiter plates were washed three times using phosphate buffered saline (PBS) with 0.05% Tween-20 and subsequently blocked with 220 µl of 5% (w/v) nonfat milk in PBS and incubated at 37°C for 1 hour. Purified 1PGE-THIVC-D7324 trimers were added at 500 ng/ml in PBS (100 µl/well) for 2-3 hours. Unbound trimers were removed by washing three times with PBS. PBS containing 3% (w/v) skimmed milk (250 µl/well) was subsequently added to block nonspecific protein-binding sites. The ELISA binding reactions were initiated by incubation of SOSIP protein to varying concentrations of mAbs for 1 hour at 37°C. After three washes with PBS, 100 µl of anti-human HRP (Jackson ImmunoResearch Laboratories Inc.) diluted at 1:2000 was added and incubated at room temperature for 50 min. The plates were further washed four times with PBS containing Triton X-100 (0.05% v/v) and color developed by addition of 100 µl of tetramethylbenzidine (TMB) substrate. Absorbance was measured at 450 nm in an ELISA reader (BioTek Inc.).

Biolayer Interferometry

For binding kinetics anti-human Fc sensors (Octet, ForteBio Inc.) were used to capture the mAbs, whereas SOSIP trimer was used as analyte in varying concentrations (ranging from 210 to 2.6 nM) in the HEPES buffer background supplemented with 0.02% Tween 20 and 0.1% BSA (pH 7.2). The binding of antigen (SOSIP) and antibody (mAbs) were carried out in room temperature by incubation of SOSIP-bound biosensors in wells containing mAbs (10 µg/ml) for 120 s with agitation at 1000 rpm. Binding association was recorded for 150 s

463 followed by dissociation for 450 s. Data were analyzed using the ForteBio Data Analysis software, 9.0 (Forte-
464 Bio Inc) and using a 1:1 binding model to fit the association and dissociation curves. A global fit was performed
465 using all curves in which the concentration of SOSIP yielded a change in binding of at least 0.1 nm and a
466 measurable dissociation.
467
468 **Differential Scanning Calorimetry (DSC)**
469 SOSIP protein in PBS (pH 7.2) diluted to 0.1- 0.2 mg/ml was loaded onto a Micro-Cal VP-Capillary DSC
470 instrument (Malvern, Inc.) and subjected to a 20 - 90 °C ramp at 60°/ h. Origin 7.0 software was used to subtract
471 baseline measurements and to fit the melting curves using a non-two-state model. Reported T_m values are for
472 the tallest peak of each sample.
473
474 **Negative stain EM**
475 1PGE-THIVC SOSIP trimers were diluted to 0.01-0.03 mg/ml, applied to a carbon coated Cu400 grid, and
476 stained with 2% (w/v) uranyl formate as described previously (19). Data were collected on an FEI Tecnai Spirit
477 T12 transmission electron microscope operating at 120 keV and equipped with a Tietz TVIPS CMOS camera.
478 A magnification of 52,000x was used, resulting in a physical pixel size at the specimen plane of 2.05 Å. Data
479 processing and analysis methods have been reported elsewhere (19). Two-dimensional classifications were
480 performed using MSA/MRA (52).
481
482 **Small Angle X-Ray Scattering (SAXS)**
483 All SAXS experiments described here have been performed on SAXSpace instrument (Anton Paar GmbH,
484 Austria). The instrument had a sealed tube X-ray source, a line collimated X-ray beam and a 1D CMOS Mythen
485 detector (Dectris, Switzerland). The wavelength of X-rays was 0.154 nm and the sample to detector distance
486 was about 317.6 mm. SAXS data was acquired on three samples of SOSIP at concentrations of 0.72, 0.85 and
487 1.1 mg/ml. For each concentration, the sample was exposed for 60 minutes (2 frames of 30 minutes each) at
488 10°C in a thermostated quartz capillary with diameter of 1 mm. The scattering data captured at detection was
489 re-calibrated for the beam position using SAXStreat software. The SAXSquant software was then used to

subtract buffer contribution, set the usable q-range, and desmear the data using the beam profile. The SAXS data was further analyzed using the programs available in the ATSAS 2.7 suite of programs (53). The radius of gyration (R_g) was calculated on the basis of automated Guinier approximation using the PRIMUSQT integrated suite of programs (54). The Porod Exponent, x was estimated by plotting $I(q)*q^x$ vs q^x till the profile resembled hyperbolic profile. The molecular mass of the scattering particles/protein molecules was calculated using the DATMOW program. Same suite was used to compute the distance distribution function in auto-mode using the program GNOM which performs an Indirect Fourier transformation on the SAXS intensity profile (55). *Ab initio* models were generated using first computing ten independent models using DAMMIF program, superimposed and averaged using SUPCOMB and DAMAVER programs, and then the averaged structure was refined using DAMMIN program. Calculations of DAMMIF were done considering no (P1) or P3 symmetry. The SAXS based model of SOSIP e19 was compared with its PDB 6B0N based homology model by inertial axes alignment of two models using SUPCOMB program. For structural visualization and figure generation, open source Pymol and UCSF Chimera programs were used.

Preparation of Env-pseudotyped viruses.

HIV-1 Env-pseudotyped viruses were prepared as described previously (32). Briefly, 293T cells were co-transfected with envelope-expressing plasmid and an *env*-deleted HIV-1 backbone plasmid (pSG3ΔEnv) using a FuGENE6 transfection kit (Promega Inc.). Cell supernatants containing pseudotyped viruses were harvested 48 h post transfection and used for infection in TZM-bl cells using DEAE-dextran (25 µg/ml) in 96-well microtiter plates. The virus infectivity titers were determined by measuring the luciferase activity using Britelite luciferase substrate (PerkinElmer Inc.) in a luminometer (Victor X2, PerkinElmer Inc.).

Site-directed mutagenesis

Point mutations by site-directed mutagenesis were introduced in *env* constructs using the QuikChange II kit (Agilent Technologies Inc.) following the manufacturer's protocol. Introduction of desired substitutions was confirmed by sequencing as described previously (32).

Neutralization assay

Neutralization assays were carried out using TZM-bl reporter cells as described before (56). Briefly, Env-pseudotyped viruses were incubated with varying dilutions of antibodies (mAbs, serum and plasma) for 1 h at 37°C in a CO_2 incubator under humidified condition. TZM-bl cells (1 X 10^4) were added into the mixture virus-antibody mixture containing 25 µg/ml DEAE-dextran (Sigma). The plates were further incubated for 48 h and the extent of virus neutralization was assessed by measuring relative luminescence units in a luminometer (Victor X2, PerkinElmer Life Sciences).

Rabbit immunization.

New Zealand white female rabbits were immunized with 30 µg of 1PE-THIVC SOSIP formulated with 40 µg Quil-A adjuvant (Invivogen Inc.) at weeks 0, 4 and 20. Four rabbits were taken in antigen immunized group and three rabbits were taken in placebo group. In placebo group, animals received PBS (pH 7.0). Pre-bled sera were obtained from all the rabbits prior to immunizations and bleed samples were collected from each animal at different time point as mentioned in Figure 6. Serum samples obtained post boost 2 were assessed for their extent to neutralize autologous and heterologous Env-pseudotyped viruses. The rabbit immunization was outsourced to a contract research organization (CRO) at Bengaluru, Karnataka, India.

Depletion of plasma and serum antibodies by monomeric gp120 and trimeric SOSIP proteins.

Purified soluble monomeric (92BR020 gp120) and trimeric 1PGE-THIVC (SOSIP gp140) proteins, in were used for the depletion of human plasma and rabbit serum neutralizing antibodies as described earlier (32). Briefly, purified gp120 and SOSIP proteins were covalently coupled to 30 mg of tosylactivated MyOne Dynabeads (Life Technologies Inc.) in coupling buffer [0.1 M $NaBO_4$,1M$(NH_4)_2SO_4$; pH 9.4] overnight at 37°C for 16 to 24 h according to the manufacturer's protocol. Env proteins bound to magnetic beads were separated from unbound proteins using a DynaMag 15 magnet (Life Technologies, Inc.). Env protein bound beads were further incubated with blocking buffer (PBS [pH 7.4], 0.1% bovine serum albumin [BSA; Sigma],

and 0.05% Tween 20) at 37°C to block the unbound sites and the antigenic integrity of Env proteins were assessed by examining their ability to bind to different mAbs by flow cytometry (FACSCanto; Becton and Dickinson, Inc.). For depletion studies, plasma and serum samples were diluted to 1:50 in Dulbecco's modified Eagle's medium (DMEM) containing 10% fetal bovine serum (FBS), and 500µl of diluted plasma or serum were incubated with 20µl of Env protein coupled magnetic beads at room temperature for 45 min. Unbound plasma and serum antibodies were separated from bound antibody fraction using a DynaMag 15 magnet as described above. This step was repeated 4 to 5 times for gp120 and 1-12 times for SOSIP protein (1PGE-THIVC) towards facilitating efficient depletion. As a negative control, G37080 plasma antibodies were depleted with uncoated beads in parallel. In addition to ELISA, the percent depletion of G37080 plasma. The degree of depletion of the polyclonal serum and plasma antibodies were assessed by ELISA and TZM-bl neutralization assay as described previously (32).

Polyclonal Fab preparation.

Serum immunoglobulin G (IgG) was purified with a mixture of protein A/G affinity column. Purified IgG was digested for 6 hours at 37° C using 4% (w/w) liquid papain (Thermo Fischer Scientific) and digestion buffer (10 mM L-cysteine, 10X EDTA, pH 8). The digestion solution was collected, and Fab fragments were purified from undigested IgG and Fc-fragments using SEC (Superdex 200 Increase; GE Healthcare). Final Fab yields were ~0.75-1.5 mg. Complexes were assembled with 10-15 μg of 1PGE-THIVC (SOSIP gp140) trimer and ~1 mg of purified polyclonal Fab, at room temperature for 18 hours. They were then purified using SEC (Superose 6 Increase; GE Healthcare) with TBS as a running buffer and concentrated with 10 kDa cutoff Amicon ultrafiltration units. Samples were diluted in TBS to ~30 μg/ml and immediately deposited onto carbon-coated 400-mesh Cu grids (glow-discharged at 15 mA for 25 s), where they were then stained with 2% (w/v) uranyl formate for 30 s. For each sample, 116,958 to 250,000 individual particle images were collected and were subsequently submitted to 2D and 3D classification using Appion (57) and Relion 3.0 (58) data processing packages. Figures were generated using UCSF Chimera (59) by aligning representative 3D

reconstructions for a specific time point and animal to each other and segmenting the maps into Fab and trimer segments. For clarity, figures only display one Fab density per epitope and a single trimer density.

DATA AND SOFTWARE AVAILABILITY.

EM volumes have been deposited to the Electron Microscopy Data Bank under accession codes EMD-22496, and EMD-22498 through EMD-22505 (inclusive) (https://www.emdataresource.org/).

Funding:

This study was made possible by funding support from the United States Agency for International Development (USAID) through IAVI, the DBT National Bioscience Research Award [grant ID: BT/ HRD/NBA34/01/2012-13(iv)], Department of Biotechnology (BT/PR24520/MED/29/1222/2017), Science & Engineering Research Board (CRG/2019/0029390), and partly by the Wellcome Trust-DBT India Alliance Team Science Grant (IA/TSG/19/1/600019) to JB; The EM work was supported by the IAVI Neutralizing Antibody Center through the Collaboration for AIDS Vaccine Discovery grants OPP1084519 (A.B.W.) and OPP1196345/INV-008813 (A.B.W.) funded by the Bill and Melinda Gates Foundation. This work was also supported by the Collaboration for AIDS Vaccine Discovery grants OPP1115782 (A.B.W.) and INV-002916 (A.B.W.) funded by the Bill and Melinda Gates Foundation. The funders had no role in study design, data collection and interpretation, or the decision to submit the work for publication.

Acknowledgements:

We thank the Protocol G study participant (G37080) registered with YRG Care, Chennai, all of the research staff members at the Protocol G clinical center at YRG Care, Chennai, and all of the IAVI Protocol G team members. We sincerely thank all our laboratory members for providing valuable input in preparing the manuscript. The 92BR020 wild type and mutant gp120 constructs as well as several bnAbs tested in this study were provided by the IAVI Neutralizing Antibody Center, the Scripps Research Institute, La Jolla, California,

USA. We also thank Prof David Montefiori for kindly providing us with the following *env* clones: Q23.17, CH038 and Q259.D22.2 used in this study. The following reagent was obtained through the NIH AIDS Reagent Program, Division of AIDS, NIAID, NIH, from John C. Kappes and Xiaoyun Wu: pSG3 env. IAVI's work was made possible by generous support from many donors, including the Bill & Melinda Gates Foundation, the Ministry of Foreign Affairs of Denmark, Irish Aid, the Ministry of Finance of Japan, the Ministry of Foreign Affairs of the Netherlands, the Norwegian Agency for Development Cooperation (NORAD), the United Kingdom Department for International Development (DFID), and the United States Agency for International Development (USAID). The full list of IAVI donors is available at www.iavi.org. The contents are the responsibility of the International AIDS Vaccine Initiative and do not necessarily reflect the views of USAID or the United States Government. We thank Prof Gagandeep Kang, Dr Rajat Goyal and Prof Sudhanshu Vrati, for support.

Author contribution:

JB conceptualized the study; JB, RK, SD, GO, A, ABW designed the study; RK, VK designed the codon optimized SOSIP and examined biophysical and biochemical properties of the Env trimer and examined antigenic and immunogenic properties and thermostability; RK performed plasma depletion assays; RK, SD carried out neutralization assays; SD, NK prepared *env* mutant constructs and mapped neutralizing antibody specificities of rabbit and human serum samples; ASC, KD, A performed SAXS analysis of Env trimer; RK, NH prepared bulk volume of 1PGE-THIVC Env and purified serum IgG for EM structural studies at TSRI; LS, GO, CAC, WL, LGH, SR, ABW carried out EMPEM analysis; SA assisted in BLI-Octet analysis; KGM, AKS identified and recruited the human elite neutralizer under IAVI Protocol G study; KGM prepared and provided the donor plasma and serum samples used in this study in addition to providing related clinical data; DS provided reagents for antibody mapping studies and helped in data analysis. JB wrote the manuscript with help from all the authors.

619

620 **Declaration of interest**:

621 A provisional patent application (201911036660) has been filed jointly by THSTI and IAVI.

Table Legends

Table 1. Neutralization of sequence matched and unmatched autologous Env-pseudotyped viruses by serum antibodies obtained from 1PGE-THIVC immunized rabbits.

Table 2. Mapping fine specificity of rabbit serum antibodies associated with neutralization of autologous virus.

Figure legends

Figure 1. Purification of 1PGE-THIVC SOSIP. 1PGE-THIVC SOSIP was purified by PGT145 antibody affinity **(A)** and size exclusion chromatography (SEC) **(B)** followed by examination through blue native gel electrophoresis (**C)**. **D.** The SEC purified two-dimensional negative-stain EM class averages of 1PGE-THIVC SOSIP.664 trimers. **E**. Efficient cleavage of 1PGE-THIVC trimeric Env observed when run in SDS-PAGE under reducing condition.

Figure 2. Antigenic properties of 1PGE-THIVC. **A**. Binding of 1PGE-THIVC with neutralizing and non-neutralizing mAbs by ELISA. **B.** Binding kinetics of 1PGE-THIVC to neutralizing and non-neutralizing mAbs by biolayer interferometry (BLI) kinetic analysis.

Figure 3. A. Effect of N279E on binding of 1PGE-THIVC with VRC01 and CD4-IgG2 by D-7324 capture ELISA. **B.** Blue native PAGE of SOSIP trimer (wild type and N27E version) in presence of 6-fold molar excess of sCD4.

Figure 4. Stability of 1 PGE-THIVC SOSIP trimer. **A**. Differential scanning calorimetry (DSC) of the SOSIP trimer; *Cp*, specific heat capacity. **B.** Time course of binding of 1PGE-THIVC to bnAbs PG9, PGT145 and a non-neutralizing mAb 39F at 37ºC.

Figure 5. A. SAXS profile of the SOSIP e19 protein at about 1 mg/ml is presented in double log mode (black symbols). The blue symbols indicate the q range used to model the P(r) curve for this protein (shown as upper inset), and the red line represents the estimated SAXS profile from the P(r) curve. Lower inset shows the Kratky plot of data (blue symbols) and modelled profile (red line). **B.** (Left column) Three rotated views of the solution shape of SOSIP e19 protein restored within shape constraints present in SAXS data are shown here. Average of ten models is shown as grey map and variation in the models is shown as black mesh map. (Middle column) Automated superimposition of the residue level model of SOSIP e19 generated using primary structure of same protein and model structure of PDB ID: 6B0N with sugar moieties, and the SAXS based model have been shown. The residue level model is shown in ribbon format with three chains are shown in blue, green and red, and sugar moieties have been shown as sticks. (Right column) The residue level models superimposed in central column are shown independently. Middle panel shows where the stem side or gp41 portion is present in the model. The red arrow highlights gap in the SAXS based model vs. residue level model near the stem or gp41 region possibly due to accessible flexibility in solution. Normalized spatial disposition (NSD) amongst ten models solved using SAXS data and χ^2 value between final averaged model vs. raw data are mentioned in bottom. **C.** Modeled structure of SOSIP e19 trimer using primary structure, SAXS data-based information and template of PDB ID: 6B0N is shown here. Three chains of gp120 are shown in red, green and blue colors. The C^{α} traces are shown as ribbons, and surfaces are shown in transparent mode. The sugar moieties representing glycosylation are shown as magenta sticks. The black arrows aid in providing the rotations done in model to present the image.

Figure 6. Immunogenicity of 1PGE-THIV in rabbits. **A.** Schedule of prime, boost and bleed time points. The binding **(B)** and neutralization of sequence matched (with and without N332) autologous viruses (**C and D**) by sera collected from four rabbits at 1:20 dilutions collected at different time points following prime and boost. **E.** Dose-dependent neutralization of pseudotyped virus expressing sequenced matched *env* (PG80v1.eJ19) by sera collected at week 22 following second boost with 1PGE-THIVC. **F.** Neutralization of pseudoviruses expressing sequence matched (PG80v1.eJ19) and unmatched (PG80v2.eJ38) autologous *envs* and heterologous tier1 *envs* (SF162 and 93IN905) by purified serum IgG in a dose-dependent manner; **G.** Binding of purified serum IgG (week 22; rabbit#1) to 1PGE-THIVC SOSIP trimer by D-7324 sandwich ELISA.

Figure 7. Effect of depletion of rabbit sera with 1PGE-THIVC SOSIP trimer on neutralization of pseudoviruses expressing sequence matched and unmatched autologous *envs*. Serum samples obtained at week 22 from best responder (rabbit#1) was depleted by incubating with purified magnetic beads coated with 1PGE-THVC trimeric Env. The depleted and undepleted serum was assessed for its ability to neutralize pseudoviruses expressing autologous *envs* by TZM-bl luciferase assay.

Figure 8. Mapping rabbit polyclonal antibody specificities by ns-EMPEM analysis. **A**. Select 2D class averages and **B.** 3D reconstructions of 1PGE-THIVC SOSIP in complex with polyclonal rabbit IgG Fab following 3 different immunization time points. For clarity, maps have been segmented into trimer (gray) and Fab (colored by epitope), and only one Fab per epitope is shown on each trimer.

Figure 9. EMPEM analysis of polyclonal IgG obtained from human elite neutralizer G37080. (**A**) Representative raw micrograph and (**B**) 2D class averages reveal a high level of heterogeneity with clusters of Fabs bound to fragments of Env, with no clear indication that intact trimers are part of these complexes. A single 2D class containing an intact trimer with no Fabs bound is circled in

orange. The remaining classes might represent trimer dissociation (classes represent free protomers with several Fabs bound), trimer opening, or a combination of both.

Supporting documents

Table S1. Mapping specificities of the autologous and heterologous plasma neutralizing antibodies obtained from the Indian elite neutralizer.

Figure S1. Different epitopes and loops in the primary structure of 1PGE-THIVC SOSIP trimer are highlighted in these images. In parentheses, highlighted residues and their respective colors are mentioned. The black arrows aid in providing the rotations done in model to present the image.

Figure S2. Alignment of C3/V4 amino acid sequences of the autologous *envs* obtained from G37080 donor. Amino acid numbering is made based on HXbc2 sequence. Amino acid residues in C3 and V4 that form key epitopes targeted by neutralizing antibodies induced in rabbits are highlighted. The glycan residue at the 362 position is underscored.

References:

1. Moore PL, Williamson C. 2016. Approaches to the induction of HIV broadly neutralizing antibodies. Curr Opin HIV AIDS 11:569-575.

2. Haynes BF. 2015. New approaches to HIV vaccine development. Curr Opin Immunol 35:39-47.

3. Gaschen B, Taylor J, Yusim K, Foley B, Gao F, Lang D, Novitsky V, Haynes B, Hahn BH, Bhattacharya T, Korber B. 2002. Diversity considerations in HIV-1 vaccine selection. Science 296:2354-60.

4. Korber B, Gnanakaran S. 2009. The implications of patterns in HIV diversity for neutralizing antibody induction and susceptibility. Curr Opin HIV AIDS 4:408-17.

5. Korber B, Hraber P, Wagh K, Hahn BH. 2017. Polyvalent vaccine approaches to combat HIV-1 diversity. Immunol Rev 275:230-244.

6. Burton DR, and D. C. Montefiori. 1997. The antibody response in HIV-1 infection. AIDS 11(Suppl. A):S87–S98.

7. Burton DR, Ahmed R, Barouch DH, Butera ST, Crotty S, Godzik A, Kaufmann DE, McElrath MJ, Nussenzweig MC, Pulendran B, Scanlan CN, Schief WR, Silvestri G, Streeck H, Walker BD, Walker LM, Ward AB, Wilson IA, Wyatt R. 2012. A Blueprint for HIV Vaccine Discovery. Cell Host Microbe 12:396-407.

8. Mascola JR, Montefiori DC. 2010. The role of antibodies in HIV vaccines. Annu Rev Immunol 28:413-44.

9. Mascola JR, Haynes BF. 2013. HIV-1 neutralizing antibodies: understanding nature's pathways. Immunol Rev 254:225-44.

10. Sanders RW, Moore JP. 2014. HIV: A stamp on the envelope. Nature 514:437-8.

11. Sanders RW, Moore JP. 2017. Native-like Env trimers as a platform for HIV-1 vaccine design. Immunol Rev 275:161-182.

12. Ward AB, Wilson IA. 2017. The HIV-1 envelope glycoprotein structure: nailing down a moving target. Immunol Rev 275:21-32.

13. Sanders RW, Derking R, Cupo A, Julien JP, Yasmeen A, de Val N, Kim HJ, Blattner C, de la Pena AT, Korzun J, Golabek M, de Los Reyes K, Ketas TJ, van Gils MJ, King CR, Wilson IA, Ward AB, Klasse PJ, Moore JP. 2013. A next-generation cleaved, soluble HIV-1 Env trimer, BG505 SOSIP.664 gp140, expresses multiple epitopes for broadly neutralizing but not non-neutralizing antibodies. PLoS Pathog 9:e1003618.

14. Sanders RW, van Gils MJ, Derking R, Sok D, Ketas TJ, Burger JA, Ozorowski G, Cupo A, Simonich C, Goo L, Arendt H, Kim HJ, Lee JH, Pugach P, Williams M, Debnath G, Moldt B, van Breemen MJ, Isik G, Medina-Ramirez M, Back JW, Koff WC, Julien JP, Rakasz EG, Seaman MS, Guttman M, Lee KK, Klasse PJ, LaBranche C, Schief WR, Wilson IA, Overbaugh J, Burton DR, Ward AB,

Montefiori DC, Dean H, Moore JP. 2015. HIV-1 VACCINES. HIV-1 neutralizing antibodies induced by native-like envelope trimers. Science 349:aac4223.

15. Sok D, Le KM, Vadnais M, Saye-Francisco KL, Jardine JG, Torres JL, Berndsen ZT, Kong L, Stanfield R, Ruiz J, Ramos A, Liang CH, Chen PL, Criscitiello MF, Mwangi W, Wilson IA, Ward AB, Smider VV, Burton DR. 2017. Rapid elicitation of broadly neutralizing antibodies to HIV by immunization in cows. Nature 548:108-111.

16. Lei L, Yang YR, Tran K, Wang Y, Chiang CI, Ozorowski G, Xiao Y, Ward AB, Wyatt RT, Li Y. 2019. The HIV-1 Envelope Glycoprotein C3/V4 Region Defines a Prevalent Neutralization Epitope following Immunization. Cell Rep 27:586-598 e6.

17. Sliepen K, Han BW, Bontjer I, Mooij P, Garces F, Behrens AJ, Rantalainen K, Kumar S, Sarkar A, Brouwer PJM, Hua Y, Tolazzi M, Schermer E, Torres JL, Ozorowski G, van der Woude P, de la Pena AT, van Breemen MJ, Camacho-Sanchez JM, Burger JA, Medina-Ramirez M, Gonzalez N, Alcami J, LaBranche C, Scarlatti G, van Gils MJ, Crispin M, Montefiori DC, Ward AB, Koopman G, Moore JP, Shattock RJ, Bogers WM, Wilson IA, Sanders RW. 2019. Structure and immunogenicity of a stabilized HIV-1 envelope trimer based on a group-M consensus sequence. Nat Commun 10:2355.

18. Sliepen K, Medina-Ramirez M, Yasmeen A, Moore JP, Klasse PJ, Sanders RW. 2015. Binding of inferred germline precursors of broadly neutralizing HIV-1 antibodies to native-like envelope trimers. Virology 486:116-20.

19. de Taeye SW, Ozorowski G, Torrents de la Pena A, Guttman M, Julien JP, van den Kerkhof TL, Burger JA, Pritchard LK, Pugach P, Yasmeen A, Crampton J, Hu J, Bontjer I, Torres JL, Arendt H, DeStefano J, Koff WC, Schuitemaker H, Eggink D, Berkhout B, Dean H, LaBranche C, Crotty S, Crispin M, Montefiori DC, Klasse PJ, Lee KK, Moore JP, Wilson IA, Ward AB, Sanders RW. 2015. Immunogenicity of Stabilized HIV-1 Envelope Trimers with Reduced Exposure of Non-neutralizing Epitopes. Cell 163:1702-15.

20. Torrents de la Pena A, Rantalainen K, Cottrell CA, Allen JD, van Gils MJ, Torres JL, Crispin M, Sanders RW, Ward AB. 2019. Similarities and differences between native HIV-1 envelope glycoprotein trimers and stabilized soluble trimer mimetics. PLoS Pathog 15:e1007920.

21. Ringe RP, Pugach P, Cottrell CA, LaBranche CC, Seabright GE, Ketas TJ, Ozorowski G, Kumar S, Schorcht A, van Gils MJ, Crispin M, Montefiori DC, Wilson IA, Ward AB, Sanders RW, Klasse PJ, Moore JP. 2019. Closing and Opening Holes in the Glycan Shield of HIV-1 Envelope Glycoprotein SOSIP Trimers Can Redirect the Neutralizing Antibody Response to the Newly Unmasked Epitopes. J Virol 93.

22. Julien JP, Lee JH, Ozorowski G, Hua Y, Torrents de la Pena A, de Taeye SW, Nieusma T, Cupo A, Yasmeen A, Golabek M, Pugach P, Klasse PJ, Moore JP, Sanders RW, Ward AB, Wilson IA. 2015. Design and structure of two HIV-1 clade C SOSIP.664 trimers that increase the arsenal of native-like Env immunogens. Proc Natl Acad Sci U S A 112:11947-52.

23. Schoofs T, Barnes CO, Suh-Toma N, Golijanin J, Schommers P, Gruell H, West AP, Jr., Bach F, Lee YE, Nogueira L, Georgiev IS, Bailer RT, Czartoski J, Mascola JR, Seaman MS, McElrath MJ, Doria-Rose NA, Klein F, Nussenzweig MC, Bjorkman PJ. 2019. Broad and Potent Neutralizing Antibodies Recognize the Silent Face of the HIV Envelope. Immunity 50:1513-1529 e9.

24. van Gils MJ, van den Kerkhof TL, Ozorowski G, Cottrell CA, Sok D, Pauthner M, Pallesen J, de Val N, Yasmeen A, de Taeye SW, Schorcht A, Gumbs S, Johanna I, Saye-Francisco K, Liang CH, Landais E, Nie X, Pritchard LK, Crispin M, Kelsoe G, Wilson IA, Schuitemaker H, Klasse PJ, Moore JP, Burton DR, Ward AB, Sanders RW. 2016. An HIV-1 antibody from an elite neutralizer implicates the fusion peptide as a site of vulnerability. Nat Microbiol 2:16199.

25. Sok D, van Gils MJ, Pauthner M, Julien JP, Saye-Francisco KL, Hsueh J, Briney B, Lee JH, Le KM, Lee PS, Hua Y, Seaman MS, Moore JP, Ward AB, Wilson IA, Sanders RW, Burton DR. 2014. Recombinant HIV envelope trimer selects for quaternary-dependent antibodies targeting the trimer apex. Proc Natl Acad Sci U S A 111:17624-9.

26. Garces F, Lee JH, de Val N, Torrents de la Pena A, Kong L, Puchades C, Hua Y, Stanfield RL, Burton DR, Moore JP, Sanders RW, Ward AB, Wilson IA. 2015. Affinity Maturation of a Potent Family of HIV Antibodies Is Primarily Focused on Accommodating or Avoiding Glycans. Immunity 43:1053-63.

27. Julien JP, Sok D, Khayat R, Lee JH, Doores KJ, Walker LM, Ramos A, Diwanji DC, Pejchal R, Cupo A, Katpally U, Depetris RS, Stanfield RL, McBride R, Marozsan AJ, Paulson JC, Sanders RW, Moore JP, Burton DR, Poignard P, Ward AB, Wilson IA. 2013. Broadly neutralizing antibody PGT121 allosterically modulates CD4 binding via recognition of the HIV-1 gp120 V3 base and multiple surrounding glycans. PLoS Pathog 9:e1003342.

28. Pauthner M, Havenar-Daughton C, Sok D, Nkolola JP, Bastidas R, Boopathy AV, Carnathan DG, Chandrashekar A, Cirelli KM, Cottrell CA, Eroshkin AM, Guenaga J, Kaushik K, Kulp DW, Liu J, McCoy LE, Oom AL, Ozorowski G, Post KW, Sharma SK, Steichen JM, de Taeye SW, Tokatlian T, Torrents de la Pena A, Butera ST, LaBranche CC, Montefiori DC, Silvestri G, Wilson IA, Irvine DJ, Sanders RW, Schief WR, Ward AB, Wyatt RT, Barouch DH, Crotty S, Burton DR. 2017. Elicitation of Robust Tier 2 Neutralizing Antibody Responses in Nonhuman Primates by HIV Envelope Trimer Immunization Using Optimized Approaches. Immunity 46:1073-1088 e6.

29. Klasse PJ, LaBranche CC, Ketas TJ, Ozorowski G, Cupo A, Pugach P, Ringe RP, Golabek M, van Gils MJ, Guttman M, Lee KK, Wilson IA, Butera ST, Ward AB, Montefiori DC, Sanders RW, Moore JP. 2016. Sequential and Simultaneous Immunization of Rabbits with HIV-1 Envelope Glycoprotein SOSIP.664 Trimers from Clades A, B and C. PLoS Pathog 12:e1005864.

30. Torrents de la Pena A, Julien JP, de Taeye SW, Garces F, Guttman M, Ozorowski G, Pritchard LK, Behrens AJ, Go EP, Burger JA, Schermer EE, Sliepen K, Ketas TJ, Pugach P, Yasmeen A, Cottrell CA, Torres JL, Vavourakis CD, van Gils MJ, LaBranche C, Montefiori DC, Desaire H, Crispin M, Klasse PJ, Lee KK, Moore JP, Ward AB, Wilson IA, Sanders RW. 2017. Improving the Immunogenicity of Native-like HIV-1 Envelope Trimers by Hyperstabilization. Cell Rep 20:1805-1817.

31. Kulp DW, Steichen JM, Pauthner M, Hu X, Schiffner T, Liguori A, Cottrell CA, Havenar-Daughton C, Ozorowski G, Georgeson E, Kalyuzhniy O, Willis JR, Kubitz M, Adachi Y, Reiss SM, Shin M, de Val N, Ward AB, Crotty S, Burton DR, Schief WR. 2017. Structure-based design of native-like HIV-1 envelope trimers to silence non-neutralizing epitopes and eliminate CD4 binding. Nat Commun 8:1655.

32. Patil S, Kumar R, Deshpande S, Samal S, Shrivastava T, Boliar S, Bansal M, Chaudhary NK, Srikrishnan AK, Murugavel KG, Solomon S, Simek M, Koff WC, Goyal R, Chakrabarti BK, Bhattacharya J. 2016. Conformational Epitope-Specific Broadly Neutralizing Plasma Antibodies

Obtained from an HIV-1 Clade C-Infected Elite Neutralizer Mediate Autologous Virus Escape through Mutations in the V1 Loop. J Virol 90:3446-57.

33. Deshpande S, Patil S, Kumar R, Shrivastava T, Srikrishnan AK, Murugavel KG, Koff WC, Chakrabarti BK, Bhattacharya J. 2016. Association of mutations in V3/C3 domain with enhanced sensitivity of HIV-1 clade C primary envelopes to autologous broadly neutralizing plasma antibodies. Retrovirology 13:41.

34. Klasse PJ, Ketas TJ, Cottrell CA, Ozorowski G, Debnath G, Camara D, Francomano E, Pugach P, Ringe RP, LaBranche CC, van Gils MJ, Bricault CA, Barouch DH, Crotty S, Silvestri G, Kasturi S, Pulendran B, Wilson IA, Montefiori DC, Sanders RW, Ward AB, Moore JP. 2018. Epitopes for neutralizing antibodies induced by HIV-1 envelope glycoprotein BG505 SOSIP trimers in rabbits and macaques. PLoS Pathog 14:e1006913.

35. McCoy LE, van Gils MJ, Ozorowski G, Messmer T, Briney B, Voss JE, Kulp DW, Macauley MS, Sok D, Pauthner M, Menis S, Cottrell CA, Torres JL, Hsueh J, Schief WR, Wilson IA, Ward AB, Sanders RW, Burton DR. 2016. Holes in the Glycan Shield of the Native HIV Envelope Are a Target of Trimer-Elicited Neutralizing Antibodies. Cell Rep 16:2327-38.

36. Ringe RP, Ozorowski G, Yasmeen A, Cupo A, Cruz Portillo VM, Pugach P, Golabek M, Rantalainen K, Holden LG, Cottrell CA, Wilson IA, Sanders RW, Ward AB, Klasse PJ, Moore JP. 2017. Improving the Expression and Purification of Soluble, Recombinant Native-Like HIV-1 Envelope Glycoprotein Trimers by Targeted Sequence Changes. J Virol 91.

37. Dey AK, David KB, Lu M, Moore JP. 2009. Biochemical and biophysical comparison of cleaved and uncleaved soluble, trimeric HIV-1 envelope glycoproteins. Virology 385:275-81.

38. Pancera M, Wyatt R. 2005. Selective recognition of oligomeric HIV-1 primary isolate envelope glycoproteins by potently neutralizing ligands requires efficient precursor cleavage. Virology 332:145-56.

39. Si Z, Phan N, Kiprilov E, Sodroski J. 2003. Effects of HIV type 1 envelope glycoprotein proteolytic processing on antigenicity. AIDS Res Hum Retroviruses 19:217-26.

40. Kumar R, Ozorowski G, Kumar V, Holden LG, Shrivastava T, Patil S, Deshpande S, Ward AB, Bhattacharya J. 2017. Characterization of a stable HIV-1 B/C recombinant, soluble, and trimeric envelope glycoprotein (Env) highly resistant to CD4-induced conformational changes. J Biol Chem 292:15849-15858.

41. Sarkar A, Bale S, Behrens AJ, Kumar S, Sharma SK, de Val N, Pallesen J, Irimia A, Diwanji DC, Stanfield RL, Ward AB, Crispin M, Wyatt RT, Wilson IA. 2018. Structure of a cleavage-independent HIV Env recapitulates the glycoprotein architecture of the native cleaved trimer. Nat Commun 9:1956.

42. Sun HX, Xie Y, Ye YP. 2009. ISCOMs and ISCOMATRIX. Vaccine 27:4388-401.

43. Ahmed FK, Clark BE, Burton DR, Pantophlet R. 2012. An engineered mutant of HIV-1 gp120 formulated with adjuvant Quil A promotes elicitation of antibody responses overlapping the CD4-binding site. Vaccine 30:922-30.

44. Ozorowski G, Cupo A, Golabek M, LoPiccolo M, Ketas TA, Cavallary M, Cottrell CA, Klasse PJ, Ward AB, Moore JP. 2018. Effects of Adjuvants on HIV-1 Envelope Glycoprotein SOSIP Trimers In Vitro. J Virol 92.

45. Bianchi M, Turner HL, Nogal B, Cottrell CA, Oyen D, Pauthner M, Bastidas R, Nedellec R, McCoy LE, Wilson IA, Burton DR, Ward AB, Hangartner L. 2018. Electron-Microscopy-Based Epitope Mapping Defines Specificities of Polyclonal Antibodies Elicited during HIV-1 BG505 Envelope Trimer Immunization. Immunity 49:288-300 e8.

46. Derking R, Allen JD, Cottrell CA, Sliepen K, Seabright GE, Lee W, Rantalainen K, Antanasijevic A, Copps J, Yasmeen A, Van der Woude P, de Taeye SW, van den Kerkhof TL, Klasse PJ, Ozorowski G, van Gils M, Moore JP, Ward AB, Crispin M, Sanders RW. 2020. Enhancing glycan occupancy of soluble HIV-1 envelope trimers to mimic the native viral spike. bioRxiv preprint https://doi.org/10.1101/2020.07.02.184135.

47. Lee JH, Leaman DP, Kim AS, Torrents de la Pena A, Sliepen K, Yasmeen A, Derking R, Ramos A, de Taeye SW, Ozorowski G, Klein F, Burton DR, Nussenzweig MC, Poignard P, Moore JP, Klasse PJ, Sanders RW, Zwick MB, Wilson IA, Ward AB. 2015. Antibodies to a conformational epitope on gp41 neutralize HIV-1 by destabilizing the Env spike. Nat Commun 6:8167.

48. Dubrovskaya V, Tran K, Ozorowski G, Guenaga J, Wilson R, Bale S, Cottrell CA, Turner HL, Seabright G, O'Dell S, Torres JL, Yang L, Feng Y, Leaman DP, Vazquez Bernat N, Liban T, Louder M, McKee K, Bailer RT, Movsesyan A, Doria-Rose NA, Pancera M, Karlsson Hedestam GB, Zwick MB, Crispin M, Mascola JR, Ward AB, Wyatt RT. 2019. Vaccination with Glycan-Modified HIV NFL Envelope Trimer-Liposomes Elicits Broadly Neutralizing Antibodies to Multiple Sites of Vulnerability. Immunity 51:915-929 e7.

49. Ruprecht CR, Krarup A, Reynell L, Mann AM, Brandenberg OF, Berlinger L, Abela IA, Regoes RR, Gunthard HF, Rusert P, Trkola A. 2011. MPER-specific antibodies induce gp120 shedding and irreversibly neutralize HIV-1. J Exp Med 208:439-54.

50. Han Q, Jones JA, Nicely NI, Reed RK, Shen X, Mansouri K, Louder M, Trama AM, Alam SM, Edwards RJ, Bonsignori M, Tomaras GD, Korber B, Montefiori DC, Mascola JR, Seaman MS, Haynes BF, Saunders KO. 2019. Difficult-to-neutralize global HIV-1 isolates are neutralized by antibodies targeting open envelope conformations. Nat Commun 10:2898.

51. Ringe RP, Sanders RW, Yasmeen A, Kim HJ, Lee JH, Cupo A, Korzun J, Derking R, van Montfort T, Julien JP, Wilson IA, Klasse PJ, Ward AB, Moore JP. 2013. Cleavage strongly influences whether soluble HIV-1 envelope glycoprotein trimers adopt a native-like conformation. Proc Natl Acad Sci U S A 110:18256-61.

52. Ogura T, Iwasaki K, Sato C. 2003. Topology representing network enables highly accurate classification of protein images taken by cryo electron-microscope without masking. J Struct Biol 143:185-200.

53. Petoukhov MV, Franke D, Shkumatov AV, Tria G, Kikhney AG, Gajda M, Gorba C, Mertens HDT, Konarev PV, Svergun DI. 2012. New developments in the ATSAS program package for small-angle scattering data analysis. Journal of Applied Crystallography 45:342-350.

54. Konarev PV, Volkov VV, Sokolova AV, Koch MHJ, Svergun DI. 2003. PRIMUS: a Windows PC-based system for small-angle scattering data analysis. Journal of Applied Crystallography 36:1277-1282.

55. Svergun DI. 1992. Determination of the Regularization Parameter in Indirect-Transform Methods Using Perceptual Criteria. Journal of Applied Crystallography 25:495-503.

56. Ringe R, Thakar M, Bhattacharya J. 2010. Variations in autologous neutralization and CD4 dependence of b12 resistant HIV-1 clade C env clones obtained at different time points from antiretroviral naive Indian patients with recent infection. Retrovirology 7:76.

57. Lander GC, Stagg SM, Voss NR, Cheng A, Fellmann D, Pulokas J, Yoshioka C, Irving C, Mulder A, Lau PW, Lyumkis D, Potter CS, Carragher B. 2009. Appion: an integrated, database-driven pipeline to facilitate EM image processing. J Struct Biol 166:95-102.

58. Zivanov J, Nakane T, Forsberg BO, Kimanius D, Hagen WJ, Lindahl E, Scheres SH. 2018. New tools for automated high-resolution cryo-EM structure determination in RELION-3. Elife 7.

59. Pettersen EF, Goddard TD, Huang CC, Couch GS, Greenblatt DM, Meng EC, Ferrin TE. 2004. UCSF Chimera--a visualization system for exploratory research and analysis. J Comput Chem 25:1605-12.

60. Mesa KA, Yu B, Wrin T, Petropoulos CJ, Pogson GH, Alexander DL, Perez G, O'Rourke SM, Sinangil F, Robinson J, Conant MA, Berman PW. 2019. Ancestral sequences from an elite neutralizer proximal to the development of neutralization resistance as a potential source of HIV vaccine immunogens. PLoS One 14:e0213409.

61. Carbonetti S, Oliver BG, Glenn J, Stamatatos L, Sather DN. 2014. Soluble HIV-1 envelope immunogens derived from an elite neutralizer elicit cross-reactive V1V2 antibodies and low potency neutralizing antibodies. PLoS One 9:e86905.

62. Wibmer CK, Bhiman JN, Gray ES, Tumba N, Abdool Karim SS, Williamson C, Morris L, Moore PL. 2013. Viral escape from HIV-1 neutralizing antibodies drives increased plasma neutralization breadth through sequential recognition of multiple epitopes and immunotypes. PLoS Pathog 9:e1003738.

63. Schommers P, Gruell H, Abernathy ME, Tran MK, Dingens AS, Gristick HB, Barnes CO, Schoofs T, Schlotz M, Vanshylla K, Kreer C, Weiland D, Holtick U, Scheid C, Valter MM, van Gils MJ, Sanders RW, Vehreschild JJ, Cornely OA, Lehmann C, Fatkenheuer G, Seaman MS, Bloom JD, Bjorkman PJ, Klein F. 2020. Restriction of HIV-1 Escape by a Highly Broad and Potent Neutralizing Antibody. Cell 180:471-489 e22.

64. LaBranche CC, Henderson R, Hsu A, Behrens S, Chen X, Zhou T, Wiehe K, Saunders KO, Alam SM, Bonsignori M, Borgnia MJ, Sattentau QJ, Eaton A, Greene K, Gao H, Liao HX, Williams WB, Peacock J, Tang H, Perez LG, Edwards RJ, Kepler TB, Korber BT, Kwong PD, Mascola JR, Acharya P, Haynes BF, Montefiori DC. 2019. Neutralization-guided design of HIV-1 envelope trimers with high affinity for the unmutated common ancestor of CH235 lineage CD4bs broadly neutralizing antibodies. PLoS Pathog 15:e1008026.

65. Lynch RM, Wong P, Tran L, O'Dell S, Nason MC, Li Y, Wu X, Mascola JR. 2015. HIV-1 fitness cost associated with escape from the VRC01 class of CD4 binding site neutralizing antibodies. J Virol 89:4201-13.

66. Seaman MS, Janes H, Hawkins N, Grandpre LE, Devoy C, Giri A, Coffey RT, Harris L, Wood B, Daniels MG, Bhattacharya T, Lapedes A, Polonis VR, McCutchan FE, Gilbert PB, Self SG, Korber BT, Montefiori DC, Mascola JR. 2010. Tiered categorization of a diverse panel of HIV-1 Env pseudoviruses for assessment of neutralizing antibodies. J Virol 84:1439-52.

67. Cao L, Pauthner M, Andrabi R, Rantalainen K, Berndsen Z, Diedrich JK, Menis S, Sok D, Bastidas R, Park SR, Delahunty CM, He L, Guenaga J, Wyatt RT, Schief WR, Ward AB, Yates JR, 3rd, Burton DR, Paulson JC. 2018. Differential processing of HIV envelope glycans on the virus and soluble recombinant trimer. Nat Commun 9:3693.

68. Nogal B, Bianchi M, Cottrell CA, Kirchdoerfer RN, Sewall LM, Turner HL, Zhao F, Sok D, Burton DR, Hangartner L, Ward AB. 2020. Mapping Polyclonal Antibody Responses in Non-human Primates Vaccinated with HIV Env Trimer Subunit Vaccines. Cell Rep 30:3755-3765 e7.

Table 1. Neutralization of sequence matched and unmatched autologous Env-pseudotyped viruses by serum antibodies obtained from 1PGE-THIVC immunized rabbits.

	Neutralization titer (ID50 values)			
Env-pseudotyped viruses	***Rabbit # 1***	***Rabbit # 2***	***Rabbit # 3***	***Rabbit # 4***
PG80v1.eJ19 WT	2284	431	104	342
PG80v1.eJ19 T332N	1081	245	<20	<20
PG80v1.eJ17	1505	194	21	169
PG80v1.eJ158	1123	178	20	103
PG80v1.eJ7	1037	141	20	161
PG80v2.eJ38	61	26	<20	234

ID50 values are reciprocal dilutions that conferred 50% neutralization of Env-pseudotyped viruses in TZM-bl cell neutralization assay.

Table 2. Mapping fine specificity of rabbit serum antibodies associated with neutralization of autologous virus.

Env constructs	ID50 values	Fold change in neutralization of Env-pseudotyped viruses	
		Fold increase	Fold decrease
PG80v1.eJ7 wild type	1798.6	-	-
PG80v1.eJ19 wild type	2117	-	-
PG80v2.eJ38 wild type	97.58	-	-
PG80v2.eJ38 (V1/V2 of v1.eJ7)	<20	No change	No change
PG80v2.eJ38 (V3/C3 of v1.eJ7)	<20	No change	No change
PG80v2.eJ38 (V3/C4 of v1.eJ7)	664.18	6.8	-
PG80v2.eJ38 (C4/C5 of v1.eJ7)	53.47	No change	-
PG80v2.eJ38 (K360R)	102.28	1.05	-
PG80v2.eJ38 (L401P)	418.46	4.3	-
PG80v2.eJ38 (N362T+K360R	181	1.85	-
PG80v2.eJ38 (N362T+L401P)	789.68	8.1	-
PG80v1.eJ7 (T362N+P401L)	101.54	-	17
PG80v1.eJ19 (T362N+P401L)	171	-	12.4
PG80v1.eJ19 (T362N)	400.72	-	5.28
PG80v1.eJ19 (P401L)	337.96	-	6.26

ID_{50} values refer to reciprocal dilution that conferred 50% neutralization of Env-pseudotyped viruses in TM-bl cells.

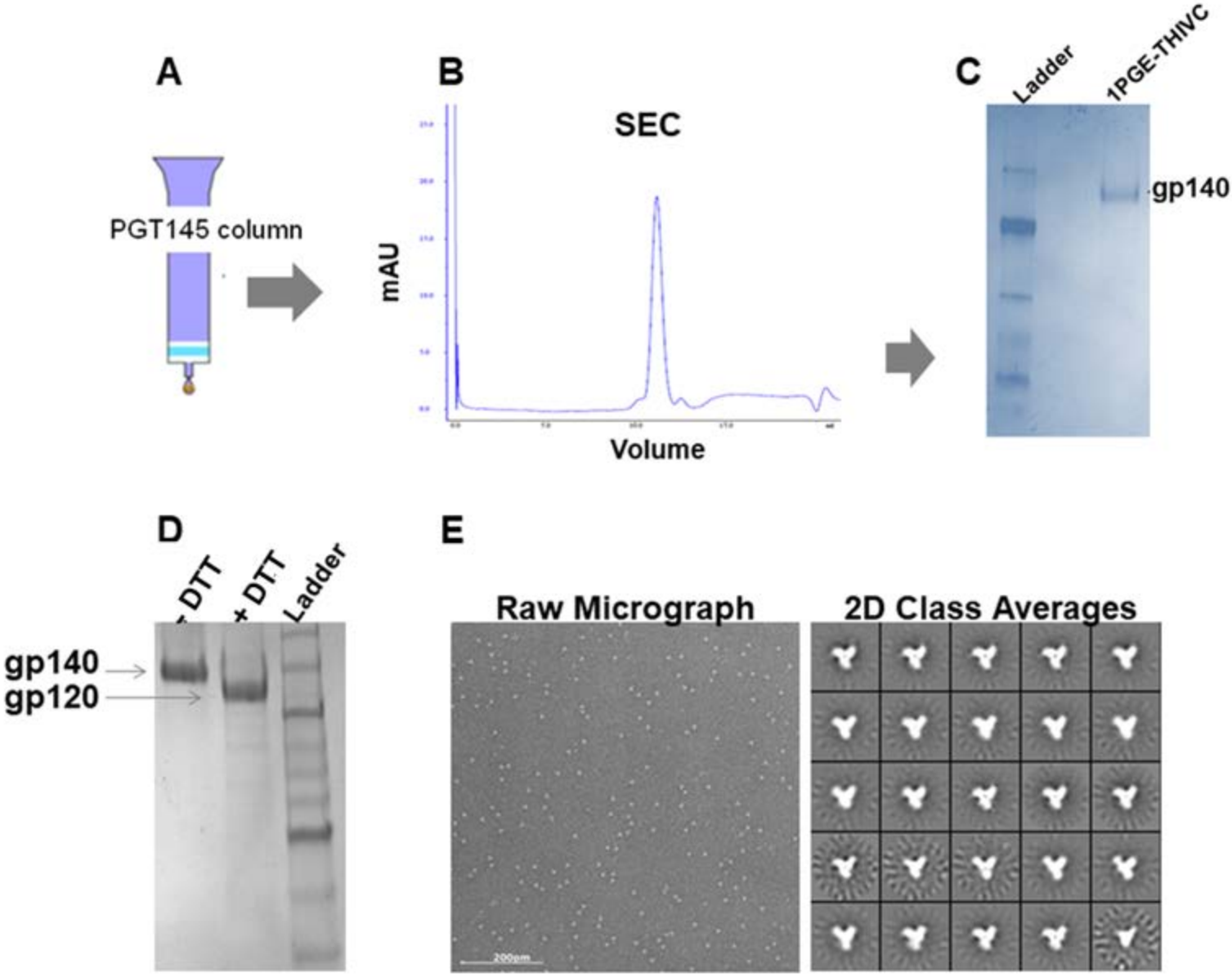
A
PGT145 column
B
SEC
mAU
Volume
C
Ladder
1PGE-THIVC
gp140
D
Ladder
gp140
gp120
E
Raw Micrograph
2D Class Averages

Figure 1

A

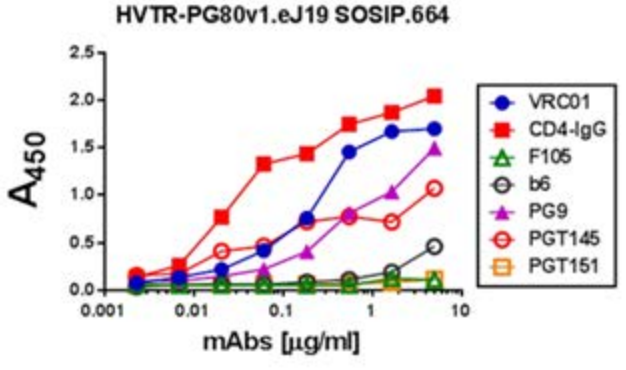

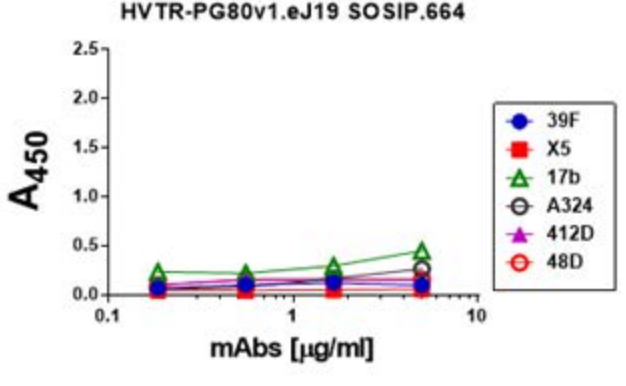

B

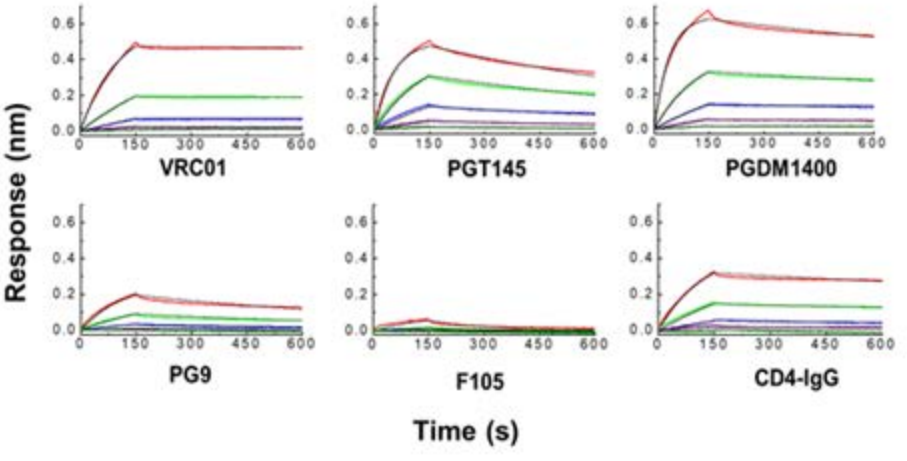

mAbs	K_D	K_{on}	K_{off}
VRC01	$1.7\pm0.7\times10^{-9}$	$5.3\pm0.8\times10^{-4}$	$0.9\pm0.4\times10^{-5}$
PGT145	$1.4\pm0.4\times10^{-8}$	$8.4\pm1.0\times10^{4}$	$1.2\pm0.2\times10^{-3}$
PGDM1400	$2.9\pm0.5\times10^{-9}$	$1.2\pm0\times10^{-5}$	$3.6\pm0.5\times10^{-4}$
PG9	$4.1\pm1.2\times10^{-8}$	$3.3\pm0.4\times10^{4}$	$1.6\pm0.9\times10^{-3}$
CD4-IgG	$5.0\pm5.6\times10^{-8}$	$3.4\pm0.3\times10^{4}$	$3.5\pm0\times10^{-4}$
F105	No Detectable Binding		

Figure 2

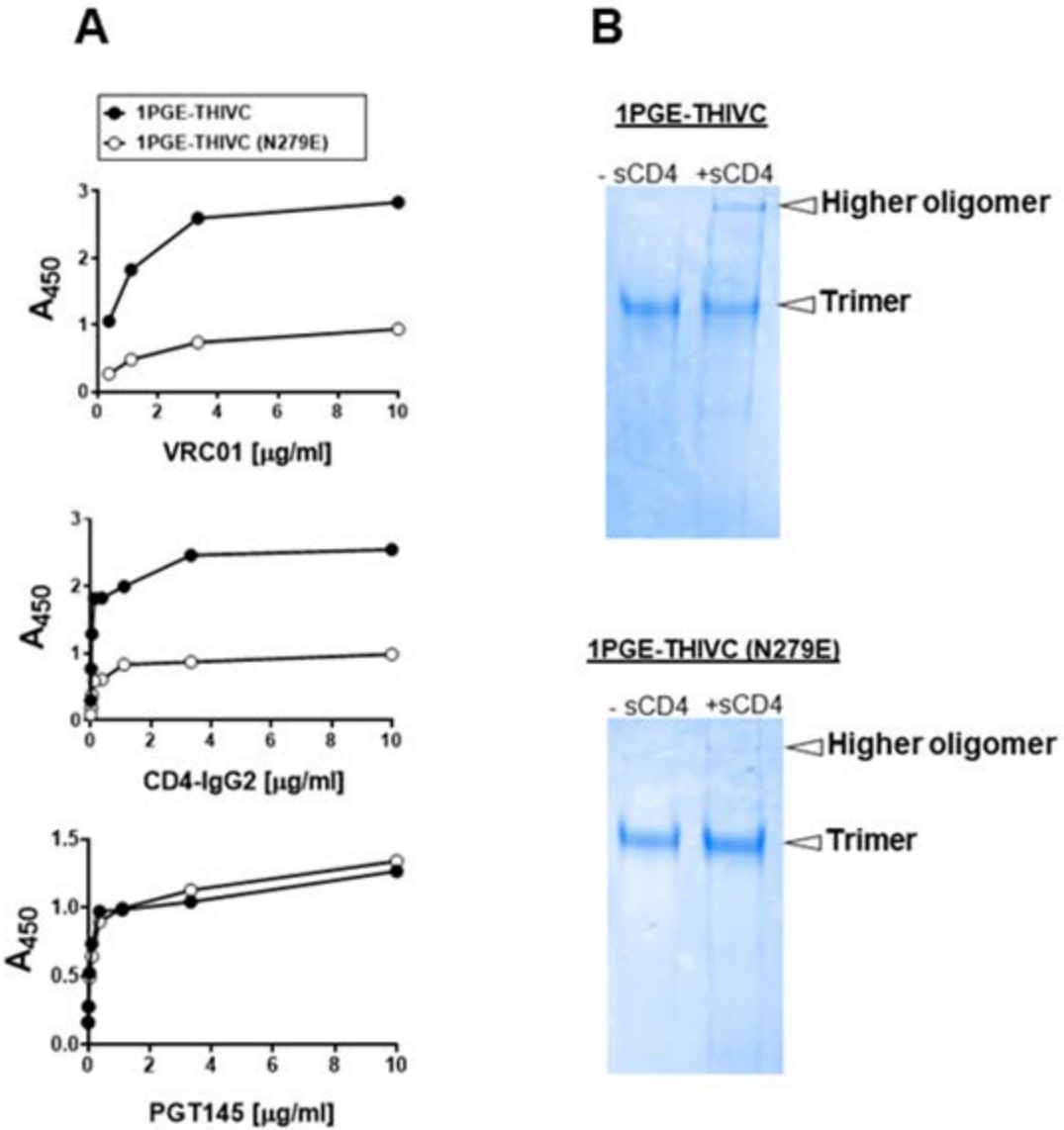
A
1PGE-THIVC
1PGE-THIVC (N279E)
A450
VRC01 [µg/ml]
CD4-IgG2 [µg/ml]
PGT145 [µg/ml]
B
1PGE-THIVC
- sCD4 +sCD4
Higher oligomer
Trimer
1PGE-THIVC (N279E)
- sCD4 +sCD4
Higher oligomer
Trimer

Figure 3

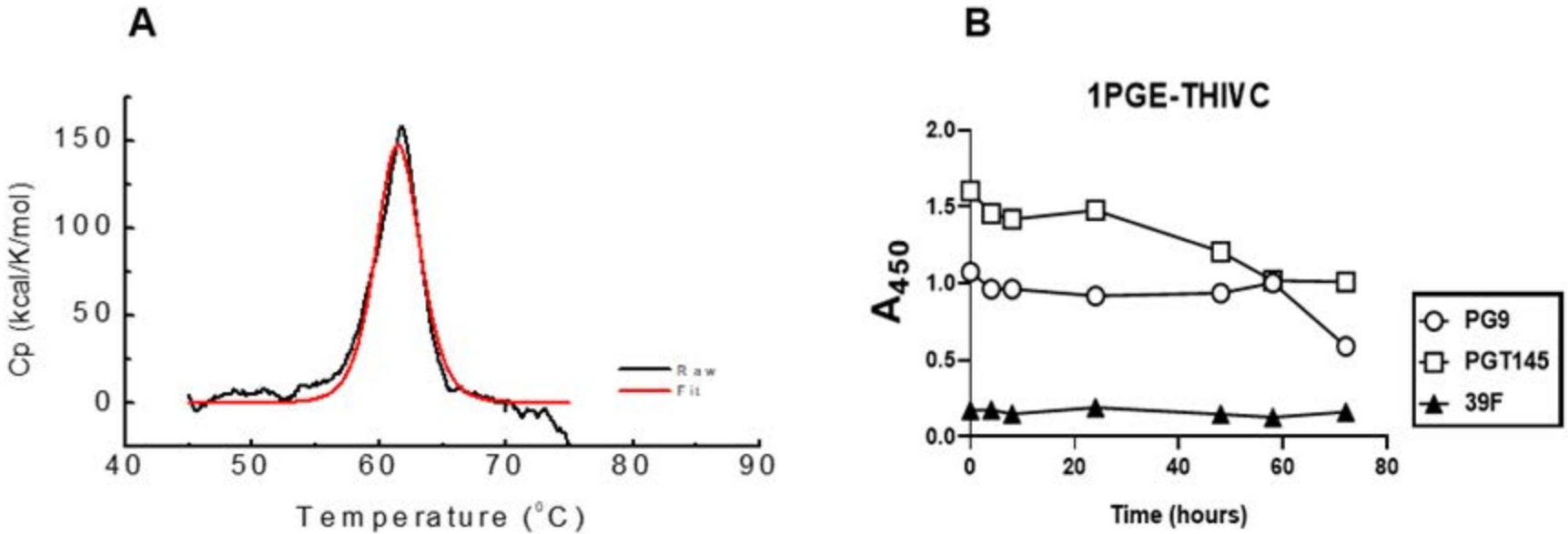
A
150
100
50
0
Cp (kcal/K/mol)
40
50
60
70
80
90
Temperature (°C)
Raw
Fit
B
1PGE-THIVC
2.0
1.5
1.0
0.5
0.0
A450
0
20
40
60
80
Time (hours)
PG9
PGT145
39F

Figure 4

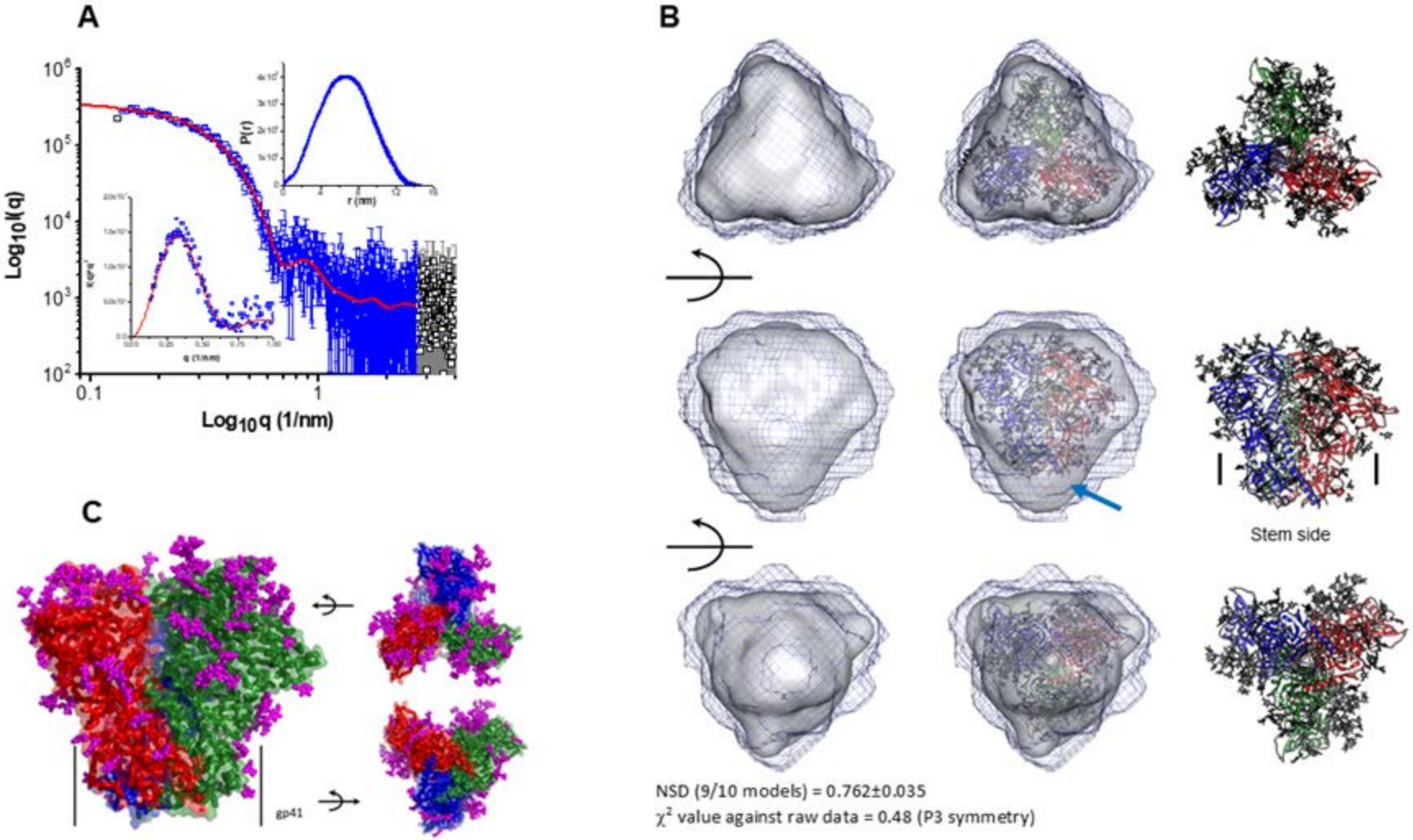
A
Log10I(q)
Log10q (1/nm)
P(r)
r (nm)
q (1/nm)
B
Stem side
NSD (9/10 models) = 0.762±0.035
χ2 value against raw data = 0.48 (P3 symmetry)
C
gp41

Figure 5

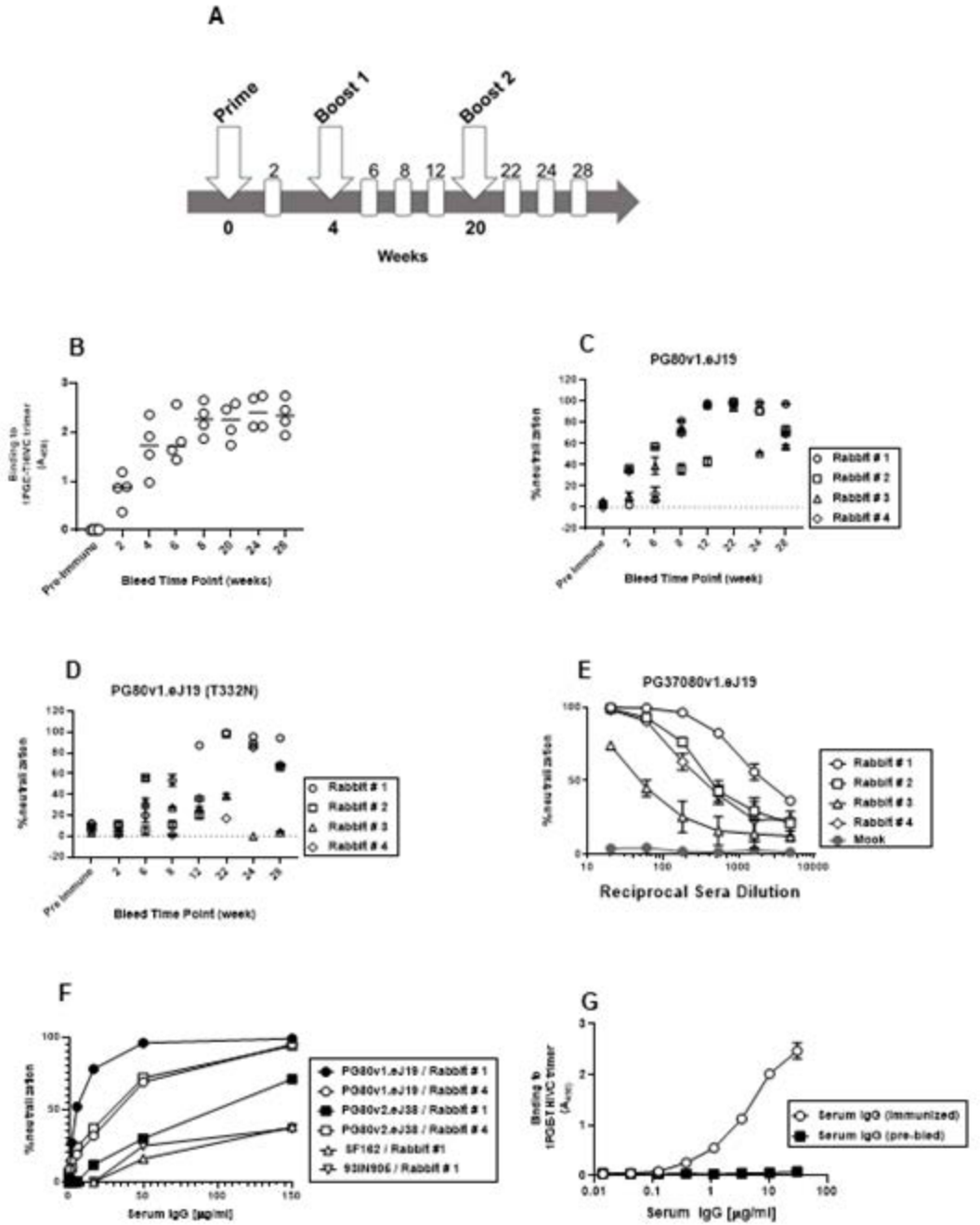
A
Prime
Boost 1
Boost 2
2
6
8
12
22
24
28
0
4
20
Weeks
B
Pre-Immune
Bleed Time Point (weeks)
C
PG80v1.eJ19
%neutralization
Rabbit # 1
Rabbit # 2
Rabbit # 3
Rabbit # 4
Bleed Time Point (week)
D
PG80v1.eJ19 (T332N)
%neutralization
Rabbit # 1
Rabbit # 2
Rabbit # 3
Rabbit # 4
Bleed Time Point (week)
E
PG37080v1.eJ19
%neutralization
Rabbit # 1
Rabbit # 2
Rabbit # 3
Rabbit # 4
Mock
Reciprocal Sera Dilution
F
%neutralization
PG80v1.eJ19 / Rabbit # 1
PG80v1.eJ19 / Rabbit # 4
PG80v2.eJ38 / Rabbit # 1
PG80v2.eJ38 / Rabbit # 4
SF162 / Rabbit #1
93IN905 / Rabbit # 1
Serum IgG [µg/ml]
G
Serum IgG (immunized)
Serum IgG (pre-bled)
Serum IgG [µg/ml]

Figure 6

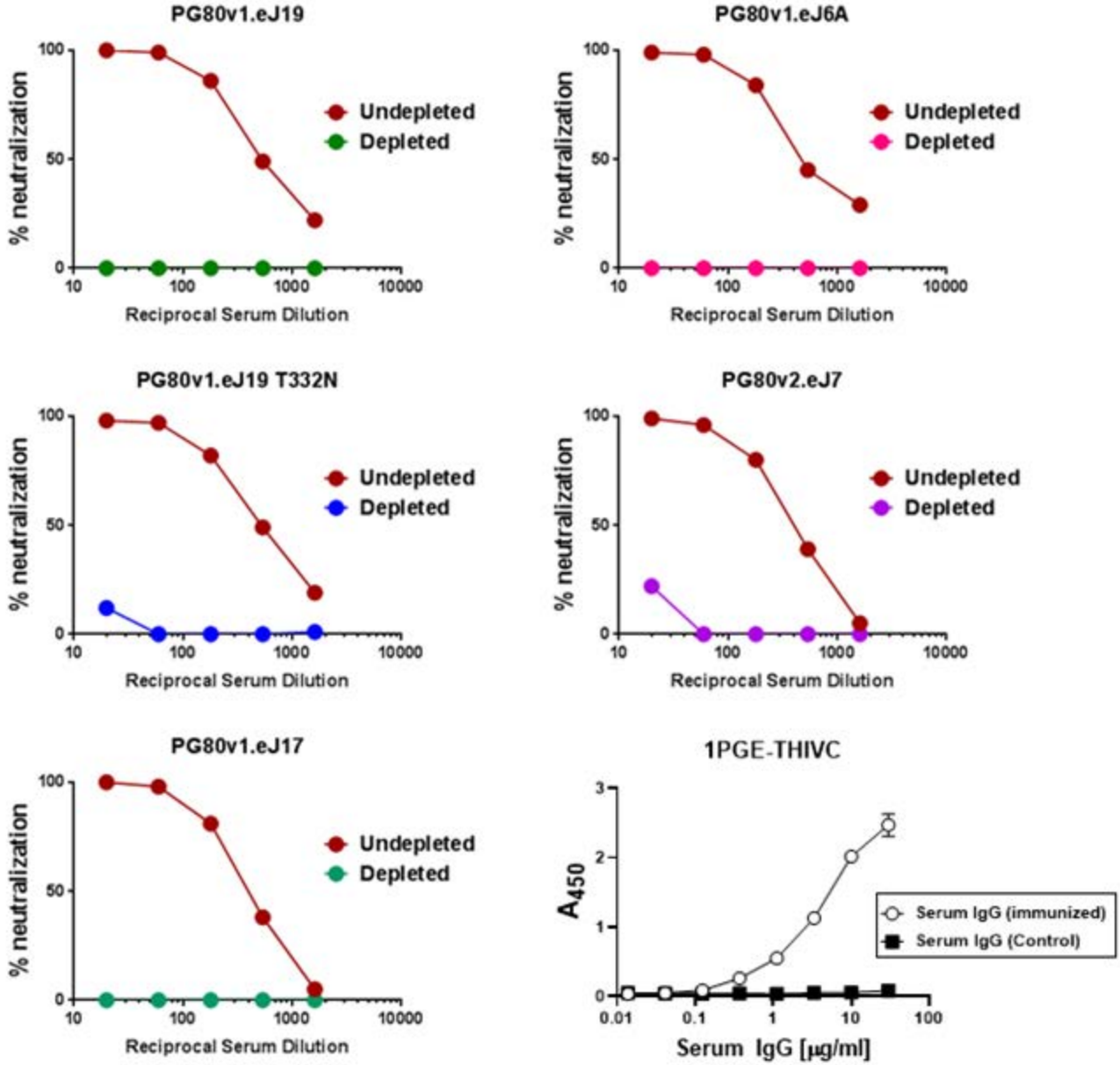
PG80v1.eJ19
% neutralization
Undepleted
Depleted
Reciprocal Serum Dilution
PG80v1.eJ6A
% neutralization
Undepleted
Depleted
Reciprocal Serum Dilution
PG80v1.eJ19 T332N
% neutralization
Undepleted
Depleted
Reciprocal Serum Dilution
PG80v2.eJ7
% neutralization
Undepleted
Depleted
Reciprocal Serum Dilution
PG80v1.eJ17
% neutralization
Undepleted
Depleted
Reciprocal Serum Dilution
1PGE-THIVC
A450
Serum IgG (immunized)
Serum IgG (Control)
Serum IgG [µg/ml]

Figure 7

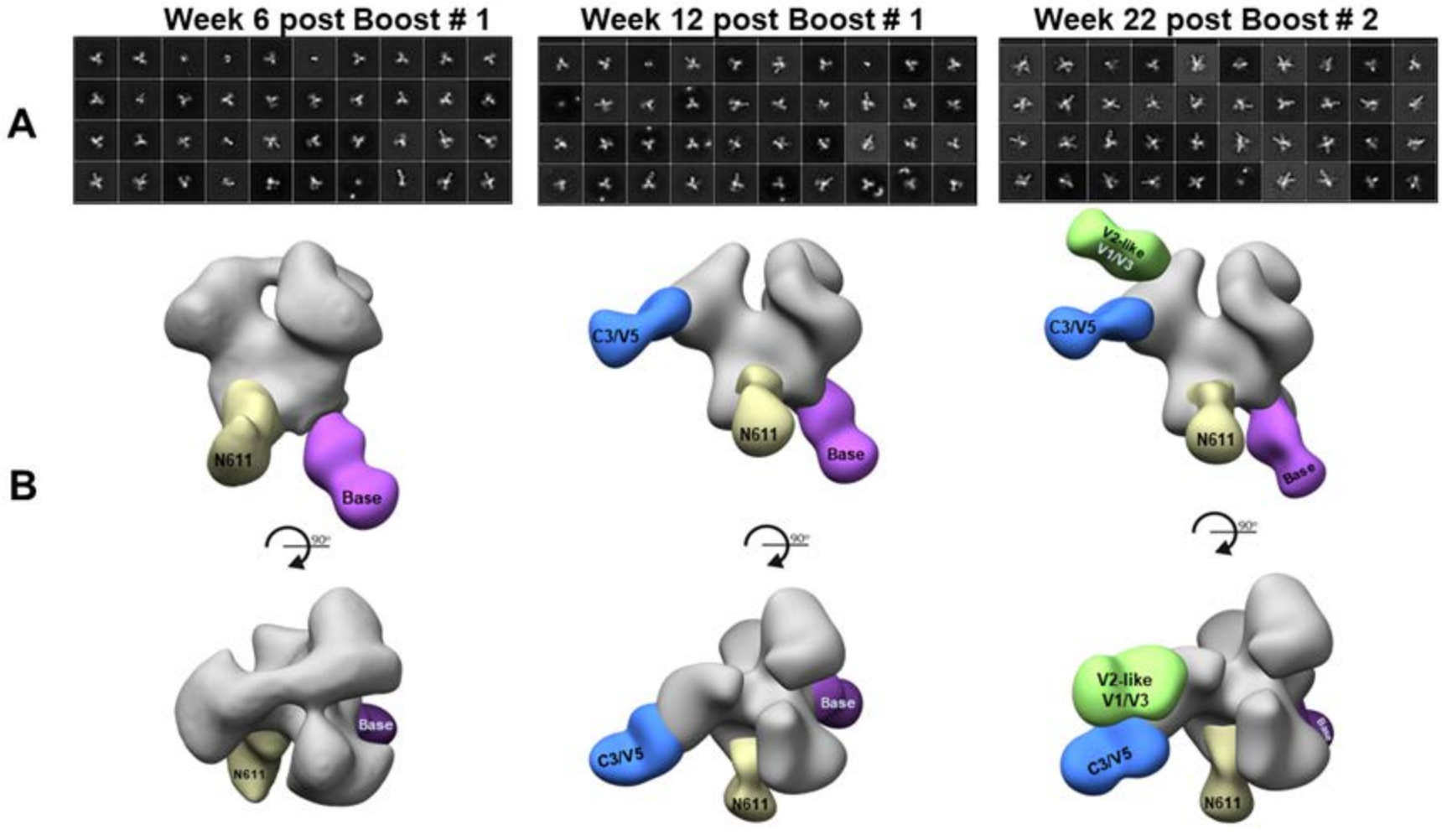
Week 6 post Boost # 1
Week 12 post Boost # 1
Week 22 post Boost # 2
A
B
N611
Base
C3/V5
V2-like
V1/V3
90°

Figure 8

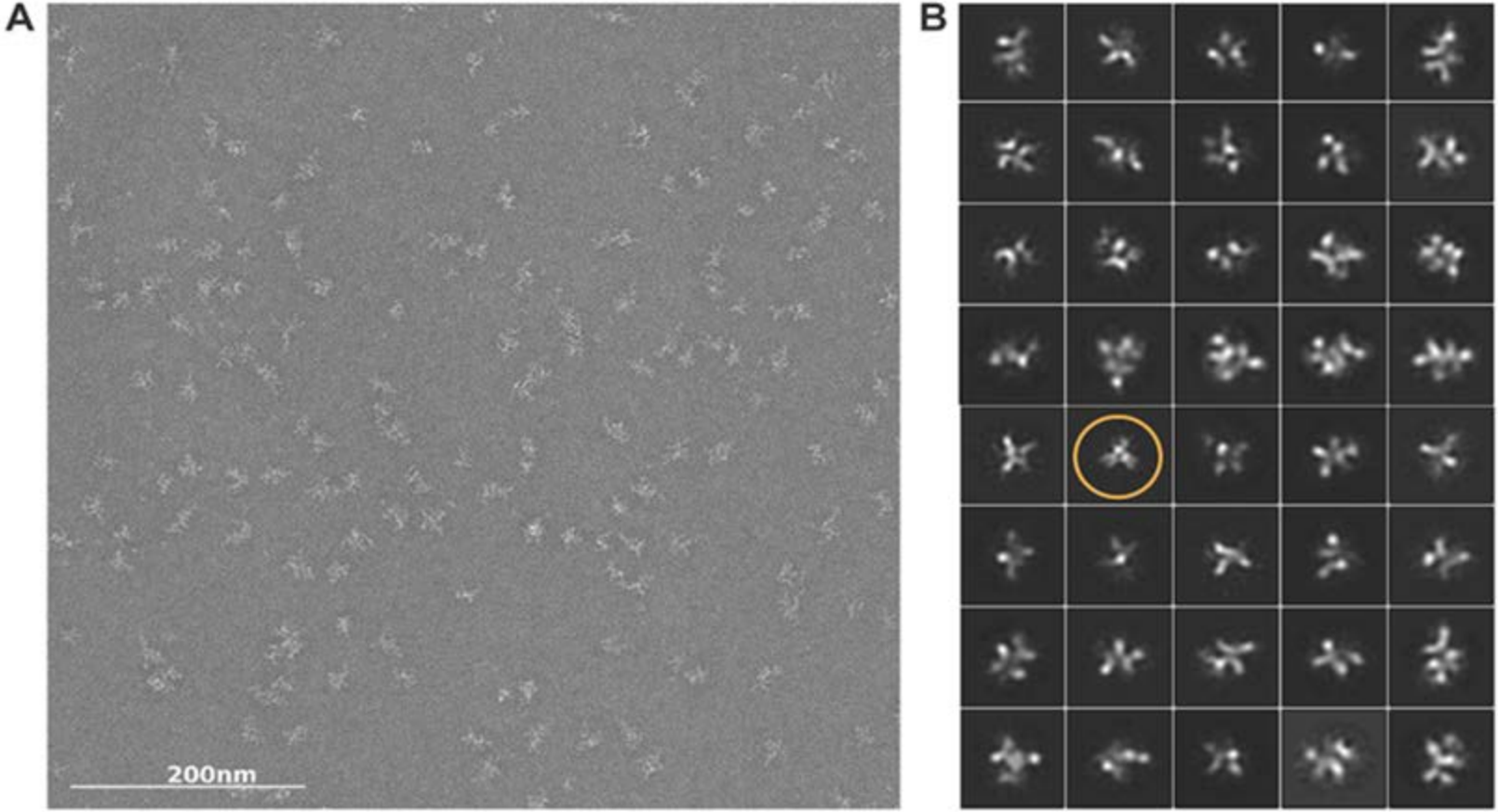

Figure 9